ISSN 2096-7071 (Print)
ISSN 2096-3101 (Online)
CN 10-1629/R1

CHINA CDC WEEKLY

Vol. 7 No. 33 Aug. 15, 2025

CCDC weekly

中国疾病预防控制中心周报

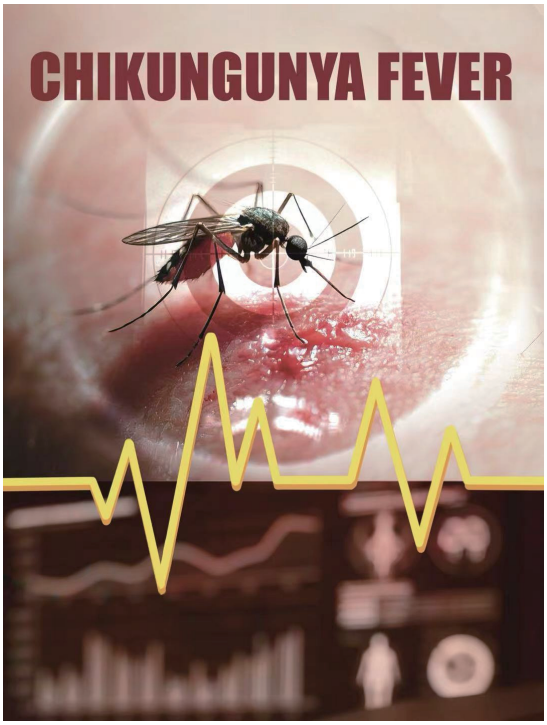

ISSN 2096-7071

China CDC Weekly

Cover Image: credited from the designer Jiaying Wang.

Preplanned Studies

Viral Load Dynamics of Chikungunya Virus in Human Specimens — Foshan City, Guangdong Province, China, 2025

Shuichun Wan[1,&]; Xin Zhang[2,&]; Xiao Cong[3,&]; Yi Liu[1]; Shen Huang[2]; Mingyi Zhou[4]; Changyun Sun[2]; Xiaofang Peng[2]; Huan Zhang[2]; Yihai Yu[1,#]; Baisheng Li[4,#]; Jianfeng He[2,#]

Summary

What is already known about this topic?

Chikungunya virus (CHIKV) represents an Aedes-borne alphavirus that causes fever, rash, and severe arthralgia. Outbreaks have expanded across 119 countries, with sporadic imported cases documented in China. While serum has been regarded as the optimal diagnostic specimen, comprehensive data comparing multiple specimen types across all infection phases have remained lacking.

What is added by this report?

Using 1,156 samples from the 2025 Foshan outbreak, we quantified CHIKV RNA levels from 6 days before to 12 days after symptom onset. Serum consistently yielded the highest viral loads, while saliva, urine, and throat swabs demonstrated inferior performance. Viral RNA detection was achievable as early as 1 day before symptom onset. Days 0–7 post-symptom onset constitute the phase of explosive viral replication, representing the optimal timeframe for specimen collection to minimize false-negative results. From Day 8 onward, antibody IgG testing should be incorporated to prevent diagnostic gaps.

What are the implications for public health practice?

Pre-symptomatic polymerase chain reaction (PCR) testing of serum (day-1) enables interception of imported cases at ports of entry; days 0–7 represent the optimal clinical sampling window to minimize false negatives. After day 8, antibody testing must supplement molecular diagnostics. This systematic analysis of CHIKV viral-load kinetics provides critical evidence for calibrating quarantine duration, optimizing contact-tracing intensity, and allocating resources effectively, thereby reducing community transmission risk substantially.

ABSTRACT

Introduction: Chikungunya virus (CHIKV), an arthropod-borne alphavirus transmitted by Aedes aegypti and Aedes albopictus, causes fever, severe joint pain, and rash. By 2025, it has triggered outbreaks in 119 countries, endangering 5.5 million people. Recent epidemics in Foshan, China, have strained healthcare systems, underscoring the need to characterize viral load dynamics across infection phases.

Methods: We collected 1,156 clinical samples from four Foshan hospitals in July 2025, spanning 6 days before to 12 days after symptom onset. Specimens included serum (904 valid), saliva (22), urine (4), throat swabs (3), and stool (37). CHIKV RNA was quantified via qRT-PCR; timepoints and specimen types with insufficient samples were excluded.

Results: Serum showed the highest positivity (90%), followed by saliva (68%), throat swabs (15%), and urine (11%); stool was negative (0%). Serum also had the highest viral loads, confirming its optimal utility. Viral RNA was detectable as early as 1 day pre-symptom onset (day-1). Days 0–7 post-onset marked explosive replication and elevated loads, representing the optimal sampling window. From Day 8 onward, loads declined, requiring IgG testing to avoid false negatives.

Conclusions: Serum is the gold standard for acute CHIKV diagnosis, with superior positivity and viral loads. Pre-symptomatic viral shedding (day-1) supports enhanced port-of-entry screening to intercept imported cases. Days 0–7 post-onset is the optimal sampling window for acute infection. During clearance (day 8+), IgG testing complements molecular diagnostics to reduce gaps. These findings inform evidence-based diagnosis, outbreak control, and resource allocation.

Chikungunya virus (CHIKV), a representative pathogen of the genus *Alphavirus* within the family Togaviridae, is primarily transmitted by *Aedes aegypti* and *Aedes albopictus* mosquitoes (*1*). As a single-

stranded, positive-sense RNA virus (ssRNA), its spherical viral particles consist of only one serotype. Based on genomic phylogenetic analysis, CHIKV can be classified into three distinct subtypes: West African, East-Central-South African (ECSA), and Asian (*2*).

The virus was initially isolated and identified in 1952 from a febrile patient in Tanzania, but large-scale epidemics began with the 2004 outbreak in Kenya, followed by a significant public health crisis on Réunion Island (France) during 2005–2006 (*3*–*5*). Over the past 20 years, Chikungunya fever has primarily persisted in sub-Saharan Africa and the tropical and subtropical regions of Southeast Asia (*4*). Prior to 2025, China documented predominantly imported cases with limited local transmission, though sporadic infections persisted. As of July 22, 2025, CHIKV transmission has expanded to 119 countries and territories, endangering approximately 5.5 million people through mosquito-borne infection and severely straining global health systems (*6*).

Typical clinical manifestations of CHIKV infection include sudden onset high fever, a maculopapular rash, and severe arthralgia (joint pain), often accompanied by myalgia (muscle pain), headache, and extreme fatigue (*7*). The incubation period typically ranges from two to 10 days (*8*), and the disease course can be clearly divided into two distinct phases: the acute phase (within the first 10 days after symptom onset) is characterized by fever (the most core symptom), arthralgia, and rash, lasting approximately seven to 10 days (*9*); this is followed by the recovery phase, during which the viral load in the patient's blood significantly decreases or becomes undetectable, and clinical symptoms gradually subside (*5*). Notably, arthritic symptoms often persist longer; while a minority of patients recover within weeks, prolonged manifestations like systemic myalgia may occur during this period (*8*).

The large-scale Chikungunya fever outbreak in Shunde District, Foshan City, Guangdong Province, China, in 2025 has drawn widespread attention (*6*,*10*), as of August 1, over 6,000 confirmed cases have been reported in the district. Currently, there are no approved specific therapeutic drugs or vaccines for this disease; clinical management relies primarily on non-steroidal anti-inflammatory drugs (NSAIDs) for symptomatic relief. At the fundamental research level, systematic spatiotemporal characterization of CHIKV infection remains incomplete, particularly the lack of integrated studies analyzing different infection phases together with tissue distribution. The relationship between viral distribution patterns among tissues and the pathological mechanisms of the acute phase also requires further clarification. Based on this knowledge gap, the present study aims to systematically elucidate the spatiotemporal transmission patterns of CHIKV by detecting its viral load and distribution characteristics in different tissues at various infection stages, thereby providing a critical theoretical foundation for investigating CHIKV pathogenicity, optimizing clinical diagnostic strategies, and developing antiviral drugs or vaccines.

During July 2025, the Guangdong Provincial Center for Disease Control and Prevention systematically collected 1,156 clinical specimens from four hospitals in Shunde District, Foshan City, Guangdong Province: Shunde First People's Hospital, Shunde Third People's Hospital, Lecong Hospital, and Chencun Hospital. Sample collection encompassed a comprehensive disease timeline spanning 6 days before to 12 days after symptom onset. To characterize CHIKV tissue distribution patterns across different infection stages, we obtained specimens from multiple anatomical sites: 1,024 blood samples, 37 stool samples, 37 urine samples, 38 saliva samples, and 20 throat swab samples. Following quality control procedures that excluded samples yielding no cycle threshold (CT) values, the final analytical dataset comprised 904 valid blood samples, 22 valid saliva samples, 4 valid urine samples, and 3 valid throat swab samples. Detection rates varied significantly across specimen types: blood demonstrated the highest positivity at 90% (923 positive of 1,024 tested), followed by saliva at 68% (26 positive of 38 tested), throat swabs at 15% (3 positive of 20 tested), and urine at 11% (4 positive of 37 tested). Notably, all fecal specimens tested negative (0 positive of 37 tested, 0% positivity rate). Specimens were systematically distributed across defined timepoints relative to symptom onset, ensuring comprehensive coverage of pre-symptomatic, acute, and convalescent phases: day -6 (1 specimen), day −1 (5 specimens), day 0 (77 specimens), day 1 (228 specimens), day 2 (296 specimens), day 3 (163 specimens), day 4 (141 specimens), day 5 (75 specimens), day 6 (51 specimens), day 7 (29 specimens), day 10 (5 specimens), day 11 (1 specimen), and day 12 (1 specimen). All patient specimens originated from individuals presenting with either mild symptoms (collected post-symptom onset) or asymptomatic

infections (collected pre-symptom onset). The entire cohort demonstrated favorable clinical outcomes following treatment, with no severe cases documented in this infection series to date.

Viral load quantification was performed using quantitative reverse transcription polymerase chain reaction (qRT-PCR). CHIKV-specific detection utilized the Chikungunya Virus Nucleic Acid Detection Kit following the manufacturer's protocol; this commercial kit does not disclose primer/probe sequences or technical specifications. The experimental workflow comprised the following standardized steps: 1) Reaction Assembly: Each 25 μL reaction mixture contained 12 μL Universal Reaction Mix, 4 μL Enzyme Master Mix, 4 μL CHIKV-Specific Primer-Probe Cocktail, and 5 μL extracted nucleic acid template. 2) Amplification Protocol: Thermal cycling conditions were as follows: reverse transcription at 50 °C for 10 minutes (1 cycle), initial denaturation at 95 °C for 5 minutes (1 cycle), followed by 40 amplification cycles consisting of denaturation at 95 °C for 10 seconds and annealing/extension at 55 °C for 40 seconds with real-time fluorescence detection in the FAM channel. All reactions included appropriate positive and negative controls, with the kit's limit of detection established at 500 copies/μL.

To determine the optimal clinical specimen for CHIKV detection across infection phases, we analyzed CT values from different specimen types collected on Days 2, 3, 4, and 5 post-symptom onset (Figure 1). Statistical analysis was restricted to timepoints with adequate sample sizes (≥3 specimens per category). Days 2 and 5 were excluded from comparative analysis due to insufficient non-serum specimens: Day 2 yielded only single samples each for saliva, throat swabs, and urine; Day 5 provided single replicates for both saliva and urine. Similarly, Day 3 throat swabs and urine specimens, and Day 4 urine samples were excluded due to inadequate sample numbers. Rigorous statistical comparison was therefore feasible only for Days 3 and 4 (Figure 1B and 1C), which revealed significantly lower viral loads in saliva compared to serum (higher CT values indicate reduced viral concentrations).

Our findings establish serum as the gold-standard specimen for clinical CHIKV RNA detection. Saliva samples cannot serve as a reliable substitute for serum in chikungunya virus diagnostics. While urine and throat swabs demonstrate detectable viral loads — albeit at substantially lower concentrations as indicated by elevated CT values — no CHIKV RNA was detected in any stool specimens. Importantly, the current viral load quantification in serum primarily reflects viral RNA levels in plasma, and we cannot entirely exclude the possibility of higher viral loads in blood cells during active viremia. As a hallmark of acute CHIKV infection, viremia encompasses not only free viral particles in plasma but also potential viral replication or sequestration within circulating blood cells — a dynamic that may contribute to overall viral persistence and transmission potential. Despite this consideration, the consistently high viral loads detected in serum confirm its position as the optimal matrix for reliable CHIKV virological testing in both clinical and public health settings.

To determine the optimal diagnostic window and minimize false-negative risks, we analyzed viral replication and clearance kinetics within the human host. We conducted a comparative analysis of valid serum samples collected at specific timepoints relative to symptom onset: −1, 0, 1, 2, 3, 4, 5, 6, 8, 9, 10, and 12 days post-symptom onset. Timepoints with fewer than three specimens were excluded from statistical analysis to ensure robust comparisons. Consequently, Day 10 and Day 12, each yielding only one specimen, were omitted from temporal analyses.

The temporal dynamics revealed distinct phases of viral activity (Figure 2). On Day −1, lower CT values indicated substantial viral loads approaching the clinical threshold, yet patients remained asymptomatic at this pre-symptomatic stage. From Day 0 through Day 5, CHIKV entered an explosive replication phase characterized by high viral loads and severe pathological symptoms. Interestingly, viral loads demonstrated a secondary increase on Days 6 and 7, confirming that Days 0–7 collectively constitute the high viral activity phase and represent the optimal period for specimen collection. Beginning on Day 8, the data exhibited greater variability with progressively fewer samples, suggesting viral entry into the recovery phase coinciding with symptom alleviation. Statistical analysis revealed significant differences in viral loads compared to Day 0 on Days 4 and 5 (P<0.05). When compared to Day 2, statistically significant differences emerged on Days 3, 4, 5, 6, and 7, with an additional significant difference observed between Days 2 and 4. These findings demonstrate clear temporal dynamics of CHIKV viremia throughout disease progression. Our analysis establishes that pre-symptomatic testing (Day −1) provides critical opportunities for screening

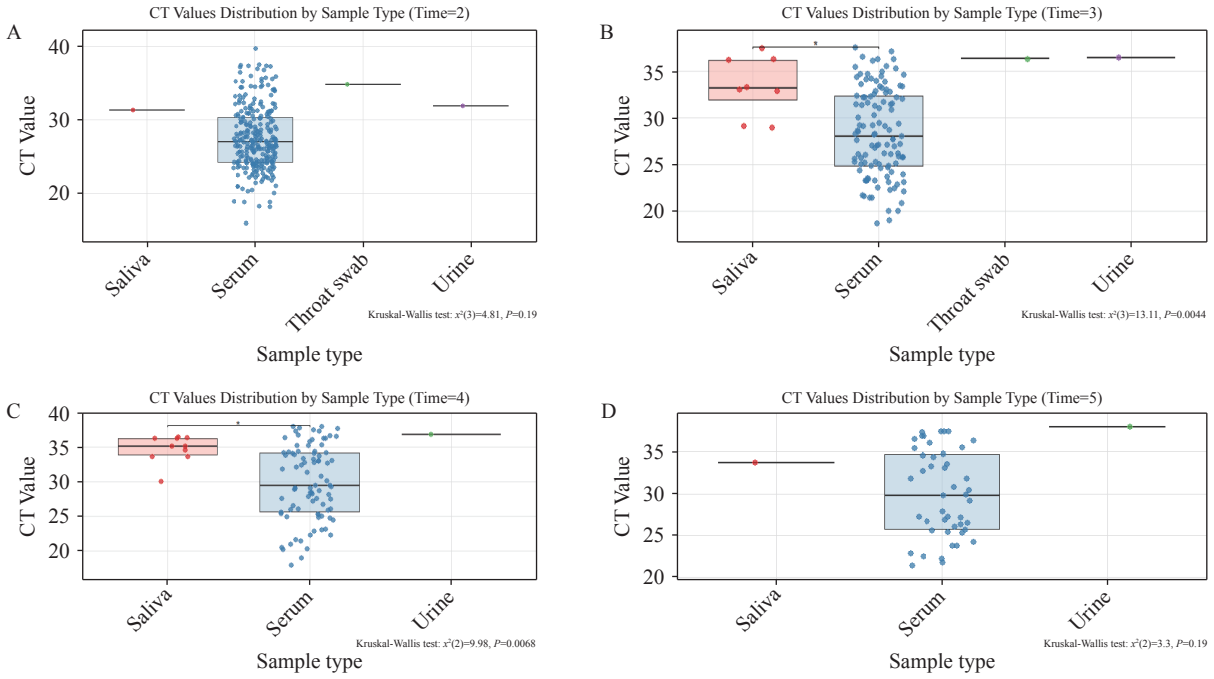

FIGURE 1. shows CT values of CHIKV nucleic acid in different specimen types on the same day representing viral loads on (A) day 2, (B) day 3, (C) day 4 and (D) day 5 post-symptom onset.
Note: For the box-and-whisker plots in these figures: The box represents the IQR, containing the middle 50% of the data. The line inside the box is the median (the 50th percentile). The whiskers extend to the minimum and maximum values within 1.5 times the IQR from the quartiles. Outliers, if present, are plotted as individual points beyond the whiskers.
Abbreviation: IQR=interquartile range; CT=cycle threshold; CHIKV=Chikungunya virus.

imported cases and high-risk contacts, while the peak viremic window (Days 0–7) represents both maximal symptom severity and the optimal timeframe for clinical sampling to minimize false negatives.

DISCUSSION

Chikungunya fever represents a significant public health challenge caused by the CHIKV, an arthropod-borne pathogen transmitted through Aedes mosquito vectors. Following transmission, infected individuals typically develop debilitating symptoms, most notably severe polyarthralgia that can persist for months beyond the acute phase (*11*).

Our comprehensive analysis of 1,156 clinical specimens collected by the Guangdong Provincial Center for Disease Control and Prevention from four hospitals in Shunde District yielded several critical insights with immediate implications for clinical practice and outbreak management. First, serum consistently demonstrated superior performance as the diagnostic specimen of choice for CHIKV detection, exhibiting substantially higher viral loads compared to alternative sample types such as saliva, urine, and throat swabs. This finding reinforces serum's established role as the gold standard for acute-phase viral diagnosis. Second, our detection of viral RNA in serum samples collected 24 hours before symptom onset represents a pivotal discovery for public health surveillance. This pre-symptomatic detectability provides a crucial window for intercepting imported cases at ports of entry and enables more effective contact tracing protocols during epidemic responses. Third, we identified Days 0–7 post-symptom onset as the optimal diagnostic window, characterized by peak viral replication and maximal detection sensitivity. Beyond Day 8, viral clearance begins, necessitating the integration of serological testing to complement molecular diagnostics and prevent false-negative results during the convalescent phase.

Several limitations warrant consideration in interpreting these findings. The restricted sample sizes for non-serum specimens (saliva, urine, throat swabs) may limit the generalizability of our comparative analyses across specimen types. Additionally, our cohort consisted primarily of mild to moderate cases, potentially limiting applicability to severe disease presentations. Future studies should incorporate larger

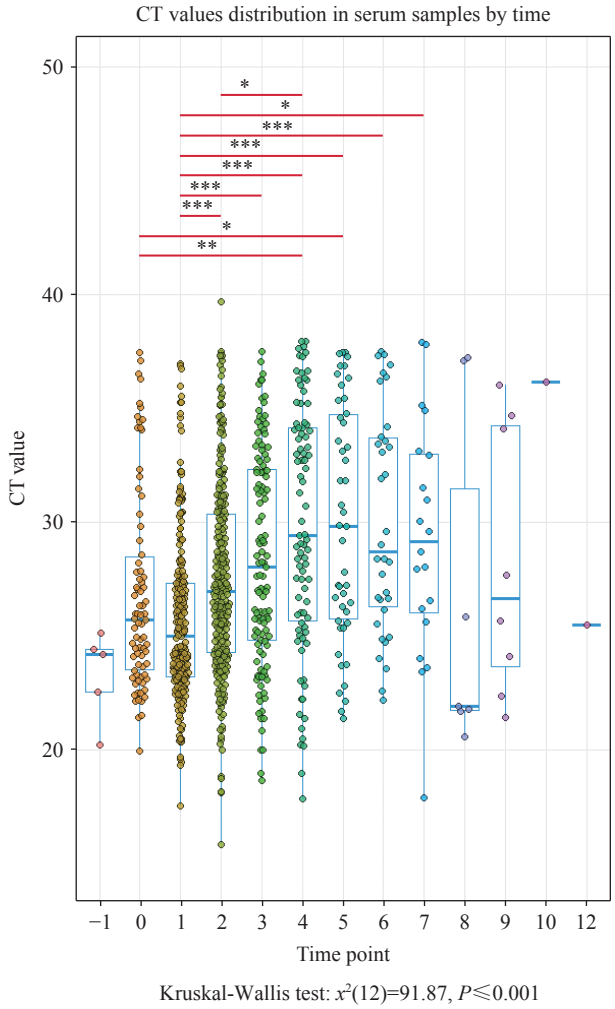

FIGURE 2. Comparison of CT values for viral nucleic acid in serum across different time points post-symptom onset.
Note: For the box-and-whisker plots in these figures: The box represents the interquartile range (IQR), containing the middle 50% of the data. The line inside the box is the median (the 50th percentile). The whiskers extend to the minimum and maximum values within 1.5 times the IQR from the quartiles. Outliers, if present, are plotted as individual points beyond the whiskers.
Abbreviation: IQR=interquartile range; CT=cycle threshold; CHIKV= Chikungunya virus.

sample sizes across all specimen types and include patients with varying disease severity to validate these temporal patterns. The practical implications of our findings extend beyond clinical diagnostics to encompass broader outbreak control strategies. The demonstration of pre-symptomatic viral detectability supports enhanced screening protocols at international borders, particularly for travelers from endemic regions. Furthermore, the clearly defined optimal sampling window (Days 0–7) enables healthcare systems to allocate diagnostic resources more efficiently while minimizing false-negative rates. These evidence-based recommendations provide a robust framework for improving both individual patient care and population-level disease surveillance during chikungunya outbreaks.

Conflicts of interest: No conflicts of interest.

Ethical statement: Approval from the Medical Research Ethics Committee of the Guangdong Provincial Center for Disease Control and Prevention under approval number W96-027E-202516.

Funding: Supported by the Guangdong Provincial Center for Disease Control and Prevention Supports Talent Projects (0720240122) and the Guangdong Provincial Key Laboratory of Pathogen Detection for Emerging Infectious Disease Response (2023B1212010010).

doi: 10.46234/ccdcw2025.182

[#] Corresponding authors: Yihai Yu, congx3@mail2.sysu.edu.cn; Baisheng Li, sjkzx_wjs@gd.gov.cn; Jianfeng He, sjkzx_hejianfeng@gd.gov.cn.

[1] Foshan Shunde 3rd People's Hospital (Foshan Shunde District Beijiao Hospital), Foshan City, Guangdong Province, China; [2] Guangdong Provincial Center for Disease Control and Prevention, Guangdong Provincial Key Laboratory of Pathogen Detection for Emerging Infectious Disease Response, Guangdong Workstation for Emerging Infectious Disease Control and Prevention, Chinese Academy of Medical Sciences, Guangzhou City, Guangdong Province, China; [3] Organ Transplant Center, the First Affiliated Hospital, Sun Yat-sen University, Guangzhou City, Guangdong Province, China; [4] School of Public Health, Sun Yat-sen University, Guangzhou City, Guangdong Province, China.
[&] Joint first authors.

Submitted: August 04, 2025
Accepted: August 12, 2025
Issued: August 15, 2025

REFERENCES

1. Freppel W, Silva LA, Stapleford KA, Herrero LJ. Pathogenicity and virulence of chikungunya virus. Virulence 2024;15(1):2396484. https://doi.org/10.1080/21505594.2024.2396484.
2. Sam IC, Kümmerer BM, Chan YF, Roques P, Drosten C, Abubakar S. Updates on chikungunya epidemiology, clinical disease, and diagnostics. Vector Borne Zoonotic Dis 2015;15(4):223 – 30. https://doi.org/10.1089/vbz.2014.1680.
3. Grandadam M, Caro V, Plumet S, Thiberge JM, Souarès Y, Failloux AB, et al. Chikungunya virus, southeastern France. Emerg Infect Dis 2011;17(5):910 – 3. https://doi.org/10.3201/eid1705.101873.
4. Cunha MS, Costa PAG, Correa IA, de Souza MRM, Calil PT, da Silva GPD, et al. Chikungunya virus: an emergent arbovirus to the South American continent and a continuous threat to the world. Front Microbiol 2020;11:1297. https://doi.org/10.3389/fmicb.2020.01297.
5. Vairo F, Haider N, Kock R, Ntoumi F, Ippolito G, Zumla A. Chikungunya: epidemiology, pathogenesis, clinical features,

management, and prevention. Infect Dis Clin North Am 2019;33(4):1003 – 25. https://doi.org/10.1016/j.idc.2019.08.006.
6. Feng Y, Chang FF, Yang Y, Lu HZ. From dengue to chikungunya: Guangdong as a sentinel for arboviral threats in East Asia. Biosci Trends 2025. https://doi.org/10.5582/bst.2025.01228.
7. Jaffar-Bandjee MC, Ramful D, Gauzere BA, Hoarau JJ, Krejbich-Trotot P, Robin S, et al. Emergence and clinical insights into the pathology of Chikungunya virus infection. Expert Rev Anti Infect Ther 2010;8(9):987 – 96. https://doi.org/10.1586/eri.10.92.
8. Singh SK, Unni SK. Chikungunya virus: host pathogen interaction. Rev Med Virol 2011;21(2):78 – 88. https://doi.org/10.1002/rmv.681.
9. Chevillon C, Briant L, Renaud F, Devaux C. The Chikungunya threat: an ecological and evolutionary perspective. Trends Microbiol 2008;16(2):80 – 8. https://doi.org/10.1016/j.tim.2007.12.003.
10. Li YH, Jiang SY, Zhang M, Li Y, He JF, Yang ZF, et al. An outbreak of Chikungunya fever in China — Foshan City, Guangdong Province, China, July 2025. China CDC Wkly, 2025;7(32):1064 – 1065 https://doi.org/10.46234/ccdcw2025.172.
11. Poh CM, Chan YH, Ng LFP. Role of T cells in Chikungunya virus infection and utilizing their potential in anti-viral immunity. Front Immunol 2020;11:287. https://doi.org/10.3389/fimmu.2020.00287.

Preplanned Studies

Genotypic Characteristics of *Mycobacterium Tuberculosis* Based on Whole Genome Sequencing — Southern Xinjiang Uygur Autonomous Region, China, 2021–2023

Palidanguli Abudureheman[1]; Senlu Wang[2]; Le Wang[2]; Gulina Badeerhan[2]; Kailibinuer Wumaier[2]; Nianqiang Liu[2]; Xiaowei Ma[1]; Xijiang Wang[2,#]

Summary

What is already known about this topic?

Currently, *Mycobacterium tuberculosis* is classified into 9 major lineages, each exhibiting distinct geographical distribution patterns and transmission characteristics. In China, Lineage 2 predominates, while Lineage 3 is primarily distributed in the Xinjiang region.

What is added by this report?

This study integrated multidimensional analyses incorporating patient characteristics, strain lineages, drug resistance profiles, and transmission networks, providing a comprehensive elucidation of *Mycobacterium tuberculosis* molecular epidemiology.

What are the implications for public health practice?

Molecular epidemiological insights into *Mycobacterium tuberculosis* transmission in Southern Xinjiang enable precision tuberculosis control.

ABSTRACT

Introduction: Southern Xinjiang Uygur Autonomous Region, China, experiences a substantial tuberculosis burden, yet comprehensive genotypic characterization of *Mycobacterium tuberculosis* strains in this region remains limited.

Methods: This study collected *Mycobacterium tuberculosis* strains and corresponding epidemiological data from patients between 2021 and 2023. Bacterial isolates underwent whole-genome sequencing using the Illumina next-generation sequencing platform. We constructed phylogenetic trees using iqtree and generated minimum spanning trees based on GraphSNP analysis, applying a clustering threshold of 12 single nucleotide polymorphisms (SNPs) to identify transmission clusters.

Results: Lineage 2 emerged as the predominant strain type, accounting for the majority of isolates, followed by Lineages 4 and 3. Notably, Lineage 2 demonstrated significantly elevated clustering rates compared to other lineages. Genetic diversity analysis revealed that Lineage 2 strains exhibited the most limited intra-lineage variation, whereas Lineage 3 displayed the greatest genetic heterogeneity among strains.

Conclusion: Our investigation demonstrates substantial genetic polymorphism among *Mycobacterium tuberculosis* strains circulating in southern Xinjiang. These findings highlight the critical need for enhanced transmission control strategies, with particular emphasis on intensive surveillance and prevention measures targeting Lineage 2 strains.

Tuberculosis (TB), a chronic infectious disease caused by *Mycobacterium tuberculosis* (MTB), continues to pose a substantial global public health challenge. According to the World Health Organization's 2023 Global TB Report, China ranked third in estimated TB incidence among 30 high-burden countries in 2022 (*1*). Within China, Xinjiang Uygur Autonomous Region has consistently maintained one of the highest tuberculosis burdens nationwide. Despite this epidemiological significance, the genotypic characteristics of circulating MTB strains in Xinjiang remain inadequately characterized. To date, nine human-adapted lineages of *Mycobacterium tuberculosis* have been identified (*2–3*), each demonstrating distinct geographical distribution patterns and unique global dissemination trajectories (*4–6*). Given Xinjiang's strategic geographical position at the crossroads of Central Asia, the region has likely developed distinctive MTB lineage characteristics that warrant comprehensive investigation.

We collected *M. tuberculosis* isolates and corresponding patient information from seven counties and cities in southern Xinjiang between 2021 and

2023. Written informed consent was obtained from all participants, and the study received approval from the central ethics review committee prior to sample collection. All isolates underwent subculturing on Lowenstein-Jensen media before DNA extraction using the cetyltrimethylammonium bromide (CTAB) method. Genomic DNA from each isolate was sequenced using Illumina PE 150 technology with 350 bp paired-end reads. For samples where the proportion of sequence classification to *Mycobacterium tuberculosis* complex (MTBC) fell below the established threshold of 90%, subsequent analytical modules were excluded to eliminate potential interference from nontuberculous mycobacteria and sample contamination.

Raw sequencing data underwent quality filtering using Fastp software. Strain identification was performed using Kraken 2, while lineage identification and drug resistance prediction were conducted using TB-Profiler. SNP detection was carried out using Samtools and bcftools. SNP differences were visualized through R-generated heatmaps, and population evolutionary analysis was performed using RAxML.

Supplementary Table S1 (available at https://weekly.chinacdc.cn/) presents the demographic characteristics of 472 isolates across population, temporal, and geographical parameters. The majority of cases (62.5%) occurred in the 56–75 age group, with a relatively balanced gender distribution (46.2% male,

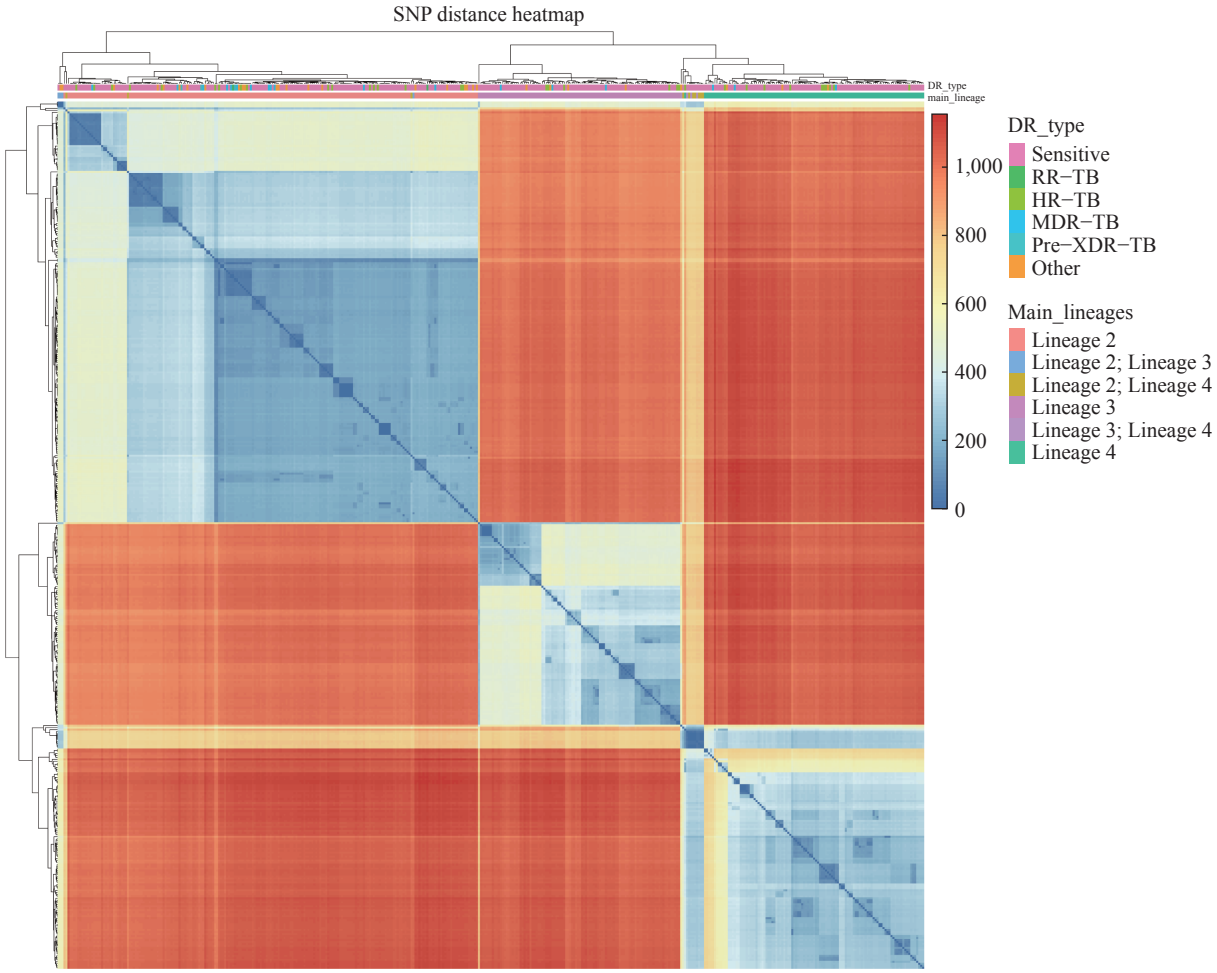

FIGURE 1. SNP distance heatmap.
Note: The hierarchical clustering dendrograms displayed on the left and top margins represent sample clustering patterns based on SNP differences. The upper panel illustrates drug resistance classifications and lineage information for each sample, with corresponding color annotations detailed in the legend. The central heatmap visualizes the SNP difference matrix, where each cell represents the SNP difference between samples corresponding to the horizontal and vertical axes. The color scale on the right indicates the magnitude of SNP differences. The heatmap clearly demonstrates the correlation patterns between lineage distributions and SNP differences.
Abbreviation: SNP=single nucleotide polymorphism.

53.8% female). Of the 472 isolates analyzed, 437 were confirmed as *M. tuberculosis*. Supplementary Table S2 (available at https://weekly.chinacdc.cn/) details the distribution of *M. tuberculosis* lineages and their respective clustering rates (SNP distance <12 served as the clustering criterion). Lineage 2 predominated (46.9%), followed by lineage 4 (25.6%) and lineage 3 (23.3%). Although lineage 2 exhibited a higher clustering rate (25.9%) compared to lineages 3 and 4 (both 19.6%), these differences were not statistically significant (χ^2=2.136, *P*=0.314).

A comprehensive heatmap was constructed to visualize SNP differences among all samples, incorporating drug resistance classifications and lineage identification data (Figure 1). Additionally, a population evolutionary tree was generated based on whole genome sequencing data, integrating lineage identification and drug resistance prediction results (Figure 2).

Figure 3 illustrates the genetic distance networks within transmission clusters. While most transmission clusters remained geographically localized, four clusters demonstrated cross-regional transmission, exemplified by the largest cluster (C1) spanning Aksu City, Wushi County, and Shache County. Among all clusters, 10 contained 22 strains exhibiting genotypic resistance.

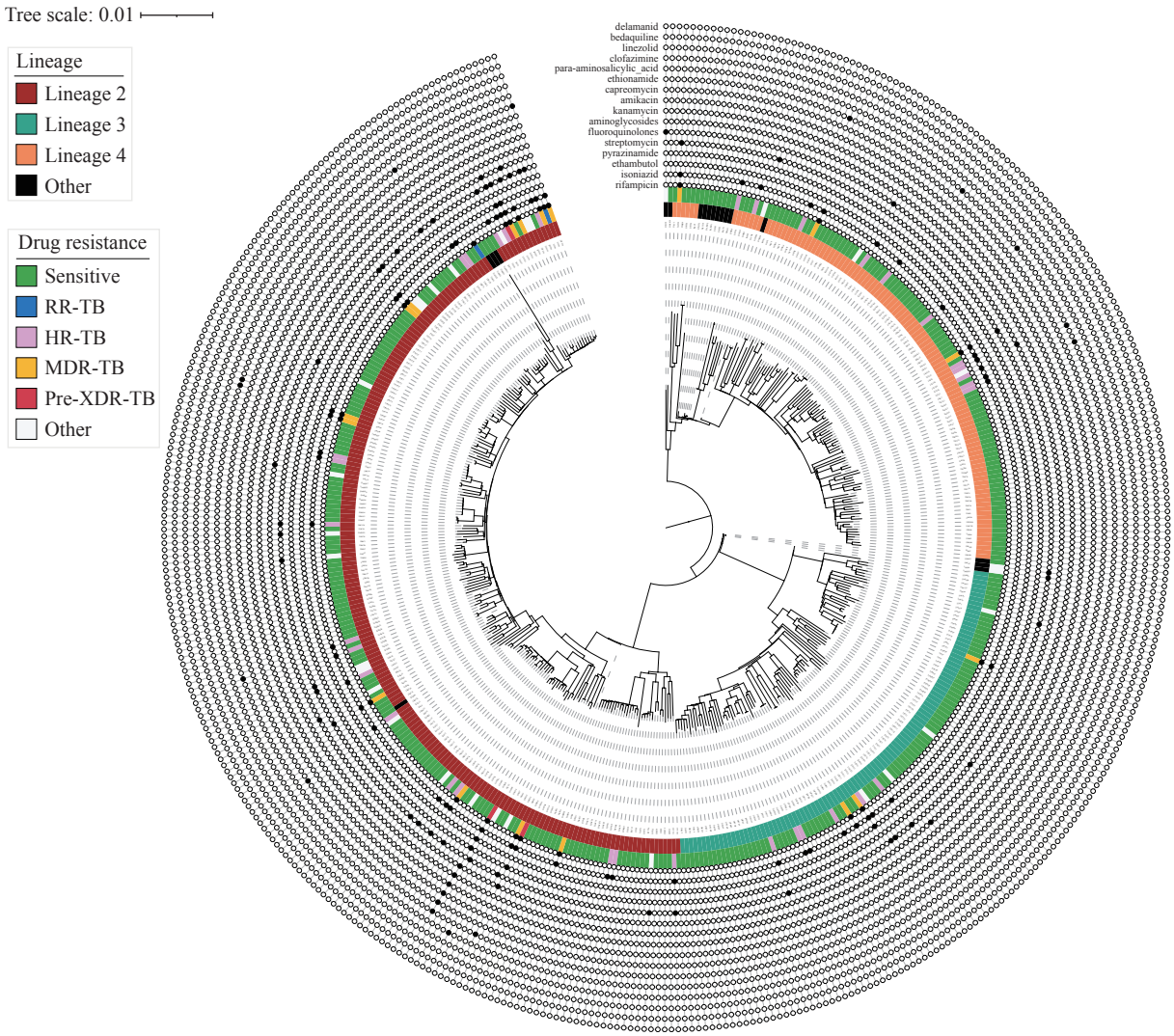

FIGURE 2. Population evolutionary tree diagram.
Note: A population evolutionary tree constructed from whole-genome sequencing SNP data of *Mycobacterium tuberculosis*, with branch lengths representing evolutionary distances. The right panel displays lineage identification and drug resistance prediction results. The color scheme for lineage identification and drug resistance classification is detailed in the legend. For individual drug resistance results, black indicates resistance while gray indicates susceptibility.
Abbreviation: SNP=single nucleotide polymorphism.

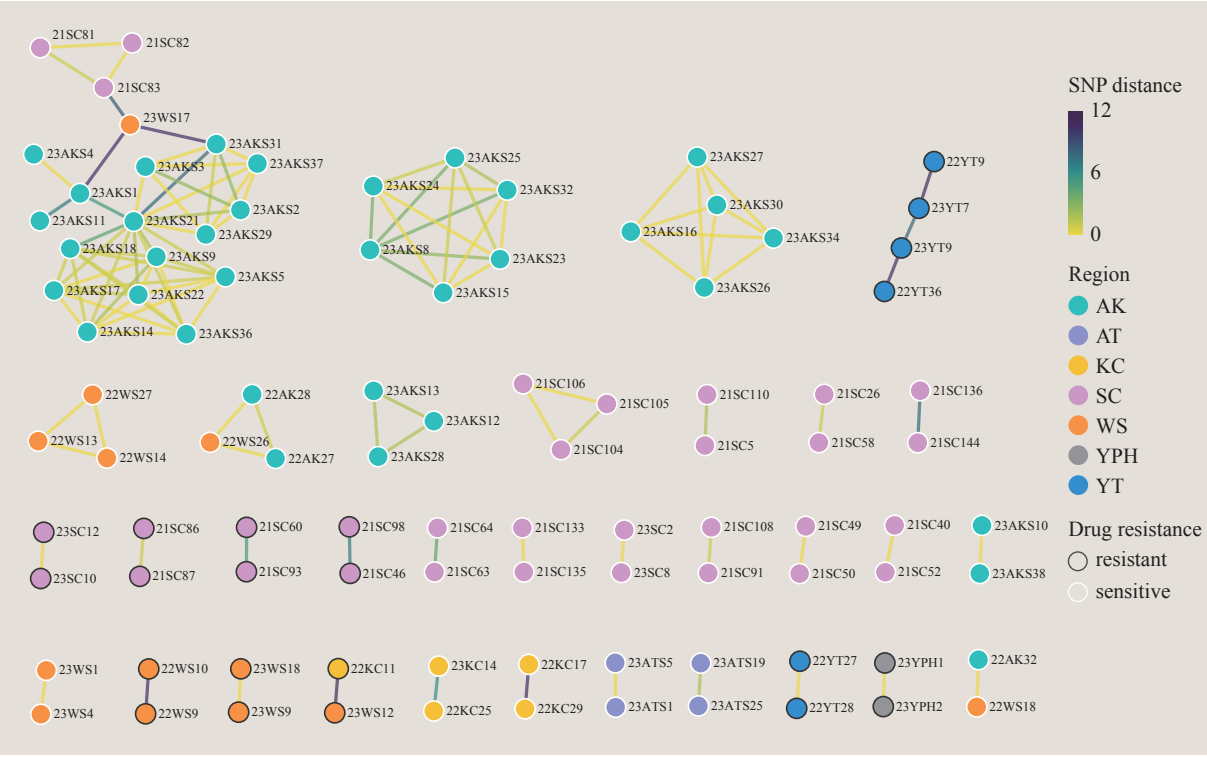

FIGURE 3. Visual network of all transmission clusters.
Note: Network visualization depicting strain relationships where individual nodes represent bacterial strains and connecting edges indicate SNP differences between strains. Node interior colors denote sampling regions, while outer ring colors indicate the presence of drug-resistance mutations. Edge colors transition from yellow to green, representing SNP differences ranging from 0 to 12.
Abbreviation: AK=Aksu; WS=Wushi; KC=Kuche; YT=Yutian; YP=Yuepuhu; SC=Shache; AT=Atushi; SNP=single nucleotide polymorphism.

Figure 4A reveals significant lineage-specific variations in genetic diversity, with lineage 2 demonstrating the lowest intra-lineage genetic variation and lineage 3 displaying the highest. Figure 4B demonstrates that while lineage 2 generally exhibits higher clustering rates, at lower thresholds (e.g., 5 SNPs), lineage 3 shows the highest clustering rate and lineage 2 the lowest. These patterns suggest sustained long-term transmission of lineage 2 in the region, whereas lineages 3 and 4 demonstrate evidence of increased recent transmission activity (within the past decade).

DISCUSSION

Understanding the molecular epidemiology of tuberculosis is essential for achieving the World Health Organization's "End TB" strategy goals. This research provides comprehensive molecular-level insights into TB transmission dynamics across southern Xinjiang, revealing important patterns that inform regional control strategies. The Beijing genotype (Lineage 2) predominates in southern Xinjiang, accounting for 46.9% of isolates. This prevalence is notably lower than previous regional studies, including reports by Yuan et al. (*7*) (57.5%) and Anwaierjiang, A et al. (*8*) (58.4%), as well as findings from northern and southern China (76.5% and 53.2%, respectively) (*9*). While Lineages 2 and 4 demonstrate widespread global distribution (*10*–*11*), our findings reflect Xinjiang's distinctive position as a historical crossroads along the ancient Silk Road Economic Belt. Notably, Lineage 3, which has been extensively documented throughout historical Silk Road regions and northwestern China (*12*), was also identified in neighboring provinces, including Tibet and Qinghai (*13*). The rapid global expansion of Lineage 2 over the past two centuries may be attributed to its enhanced transmission capacity and propensity for drug resistance development, which correlates with the higher clustering rate observed for Lineage 2 in our study (*14*).

Genetic distance analysis enables precise characterization of tuberculosis transmission patterns and identification of potential multiple transmission

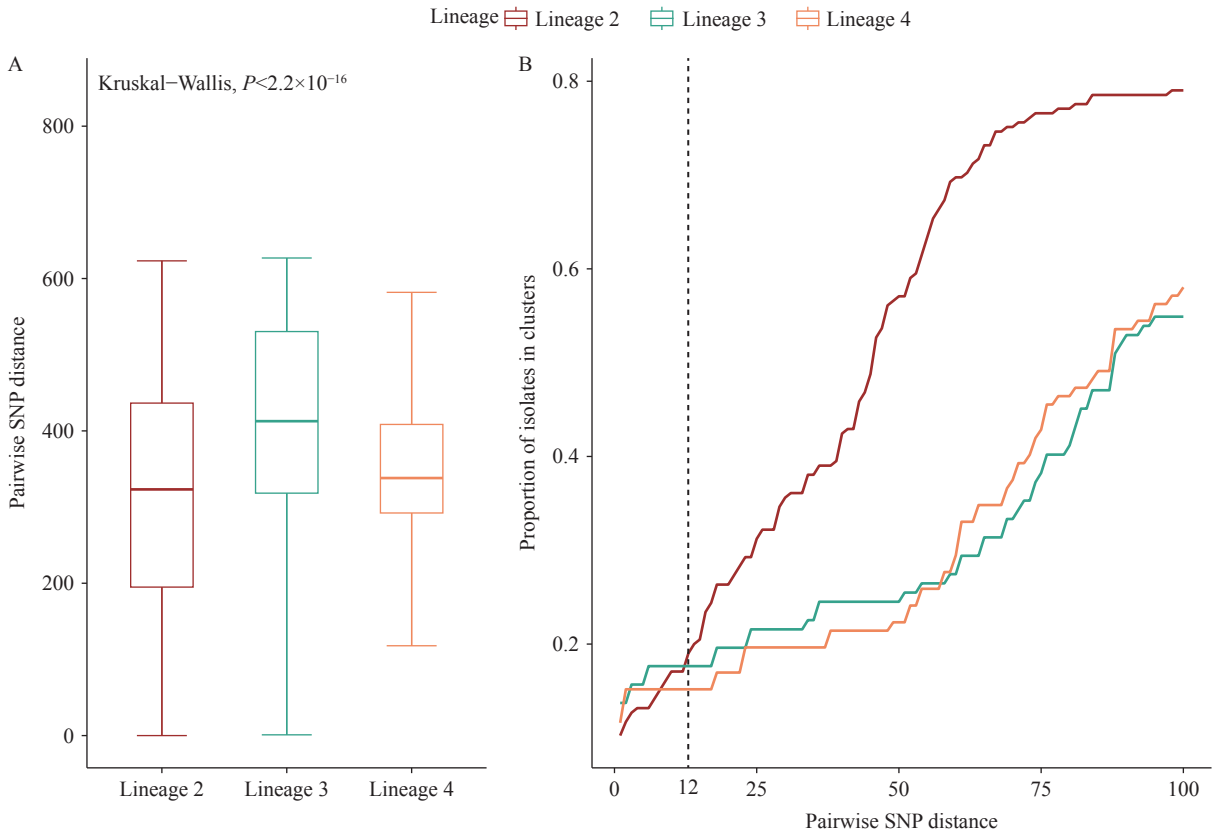

FIGURE 4. Comparison of genetic distance and clustering among different lineages. (A) Box plot distribution of inter-strain SNP differences across the three lineages. (B) Cumulative clustering ratio curves for the three bacterial lineages using varying SNP difference thresholds (1–100) for transmission clustering.
Note: For (B), the clustering rates at different thresholds reflect lineage-specific clustering patterns and indirectly indicate transmission scales across different time periods.

sources within communities. The overall clustering rate of 22.2% observed in southern Xinjiang approximates that reported in Shanghai (25.2%) while substantially exceeding rates documented in Shenzhen (12.2%) (*15–16*). Our investigation revealed mixed lineage infections across all seven studied counties and cities, indicating elevated levels of recent transmission activity. This transmission pattern likely reflects the complex interplay of local cultural practices, housing conditions, and socioeconomic determinants that facilitate disease spread, warranting comprehensive epidemiological investigation.

As Xinjiang assumes an increasingly pivotal role in China's Belt and Road Initiative, expanding economic cooperation and human mobility with the five Central Asian republics necessitates enhanced infectious disease surveillance systems. This evolving landscape demands strengthened international collaboration in tuberculosis control, particularly through research and development of innovative diagnostic technologies, targeted support for border regions, and establishment of robust cross-border prevention mechanisms. Such coordinated multilateral efforts are fundamental to achieving the ambitious "End TB" strategy objectives by 2030. Future research should incorporate larger sample sizes and extended temporal frameworks to strengthen these preliminary findings and guide evidence-based policy development.

Conflicts of interest: No conflicts of interest.

Acknowledgements: Dr. Wang Xiaoyin's team at the Zhejiang Provincial Center for Disease Control and Prevention for their invaluable contributions. The essential support and assistance provided by the Centers for Disease Control and Prevention in Kashgar, Hotan, Kezhou, and Aksu regions.

Funding: Supported by the "Tianshan Talents" Medical and Health High-level Talent Training Program (TSYC202301B166), the Natural Science Foundation of Xinjiang Uygur Autonomous Region Project (2023D01C57), and grant WJW2024-087.

doi: 10.46234/ccdcw2025.181

[#] Corresponding author: Xijiang Wang, wxj@xjcdc.com.

[1] School of Public Health, Xinjiang Medical University, Urumqi City, Xinjiang Uygur Autonomous Region, China; [2] Xinjiang Uygur Autonomous Region Center for Disease Control and Prevention, Urumqi City, Xinjiang Uygur Autonomous Region, China.

Submitted: January 01, 2025
Accepted: July 27, 2025
Issued: August 15, 2025

REFERENCES

1. Bagcchi S. WHO's global tuberculosis report 2022. Lancet Microbe 2023;4(1):e20. https://doi.org/10.1016/S2666-5247(22)00359-7.
2. Ngabonziza JCS, Loiseau C, Marceau M, Jouet A, Menardo F, Tzfadia O, et al. A sister lineage of the *Mycobacterium tuberculosis* complex discovered in the African Great Lakes region. Nat Commun 2020;11(1):2917. https://doi.org/10.1038/s41467-020-16626-6.
3. Coscolla M, Gagneux S, Menardo F, Loiseau C, Ruiz-Rodriguez P, Borrell S, et al. Phylogenomics of *Mycobacterium africanum* reveals a new lineage and a complex evolutionary history. Microb Genom 2021;7(2):000477. https://doi.org/10.1099/mgen.0.000477.
4. Gagneux S, DeRiemer K, Van T, Kato-Maeda M, de Jong BC, Narayanan S, et al. Variable host-pathogen compatibility in *Mycobacterium tuberculosis*. Proc Natl Acad Sci USA 2006;103(8):2869 – 73. https://doi.org/10.1073/pnas.0511240103.
5. Pasipanodya JG, Moonan PK, Vecino E, Miller TL, Fernandez M, Slocum P, et al. *Allopatric* tuberculosis host-pathogen relationships are associated with greater pulmonary impairment. Infect Genet Evol 2013;16:433 – 40. https://doi.org/10.1016/j.meegid.2013.02.015.
6. Stucki D, Brites D, Jeljeli L, Coscolla M, Liu QY, Trauner A, et al. *Mycobacterium tuberculosis* lineage 4 comprises globally distributed and geographically restricted sublineages. Nat Genet 2016;48(12):1535 – 43. https://doi.org/10.1038/ng.3704.
7. Yuan L, Mi LG, Li YX, Zhang H, Zheng F, Li ZY. Genotypic characteristics of *Mycobacterium tuberculosis* circulating in Xinjiang, China. Infect Dis 2016;48(2):108 – 15. https://doi.org/10.3109/23744235.2015.1087649.
8. Anwaierjiang A, Wang Q, Liu HC, Yin CJ, Xu M, Li MC, et al. Prevalence and molecular characteristics based on whole genome sequencing of *Mycobacterium tuberculosis* resistant to four anti-tuberculosis drugs from southern Xinjiang, China. Infect Drug Resist 2021;14:3379 – 91. https://doi.org/10.2147/IDR.S320024.
9. Pang Y, Zhou Y, Zhao B, Liu G, Jiang GL, Xia H, et al. Spoligotyping and drug resistance analysis of *Mycobacterium tuberculosis* strains from national survey in China. PLoS One 2012;7(3):e32976. https://doi.org/10.1371/journal.pone.0032976.
10. Gagneux S. Ecology and evolution of *Mycobacterium tuberculosis*. Nat Rev Microbiol 2018;16(4):202 – 13. https://doi.org/10.1038/nrmicro.2018.8.
11. Comas I, Coscolla M, Luo T, Borrell S, Holt KE, Kato-Maeda M, et al. Out-of-Africa migration and Neolithic coexpansion of *Mycobacterium tuberculosis* with modern humans. Nat Genet 2013;45(10):1176 – 82. https://doi.org/10.1038/ng.2744.
12. Zhou Y, van den Hof S, Wang SF, Pang Y, Zhao B, Xia H, et al. Association between genotype and drug resistance profiles of *Mycobacterium tuberculosis* strains circulating in China in a national drug resistance survey. PLoS One 2017;12(3):e0174197. https://doi.org/10.1371/journal.pone.0174197.
13. O'Neill MB, Shockey A, Zarley A, Aylward W, Eldholm V, Kitchen A, et al. Lineage specific histories of *Mycobacterium tuberculosis* dispersal in Africa and Eurasia. Mol Ecol 2019;28(13):3241 – 56. https://doi.org/10.1111/mec.15120.
14. Merker M, Blin C, Mona S, Duforet-Frebourg N, Lecher S, Willery E, et al. Evolutionary history and global spread of the *Mycobacterium tuberculosis* Beijing lineage. Nat Genet 2015;47(3):242 – 9. https://doi.org/10.1038/ng.3195.
15. Li M, Lu LP, Jiang Q, Jiang Y, Yang CG, Li J, et al. Genotypic and spatial analysis of transmission dynamics of tuberculosis in Shanghai, China: a 10-year prospective population-based surveillance study. Lancet Reg Health West Pac 2023;38:100833. https://doi.org/10.1016/j.lanwpc.2023.100833.
16. Yang TT, Wang YX, Liu QY, Jiang Q, Hong CY, Wu LK, et al. A population-based genomic epidemiological study of the source of tuberculosis infections in an emerging city: Shenzhen, China. Lancet Reg Health West Pac 2021;8:100106. https://doi.org/10.1016/j.lanwpc.2021.100106.

SUPPLEMENTARY MATERIAL

SUPPLEMENTARY TABLE S1. Demographic characteristics of the 472 isolates in Xinjiang Uygur Autonomous Region, China.

Variables	No. of patients	Constituent ratio (%)
Age (Years)		
<25	27	5.7
26–55	83	17.6
56–75	295	62.5
>75	67	14.2
Sex		
Male	218	46.2
Female	254	53.8
Year		
2021	143	30.3
2022	148	31.4
2023	181	38.3
Region		
Aksu	70	14.8
Kuche	60	12.7
Wushi	59	12.5
Shache	165	35.0
Yuepuhu	21	4.4
Yutian	62	13.1
Atushi	35	7.4

SUPPLEMENTARY TABLE S2. Distribution of lineages and clustering rates among *M. tuberculosis* strains.

Lineages	No. of isolates (constituent ratio)	No. of cases in cluster (clustering rate)	χ^2	*P*
Lineage 2	205 (46.9%)	53 (25.9%)	2.136	0.314
Lineage 3	102 (23.3%)	20 (19.6%)		
Lineage 4	112 (25.6%)	22 (19.6%)		

Vital Surveillances

Epidemiological Characteristics of Tuberculosis Among Interprovincial Migrants — China, 2019–2023

Da Xu[1,2]; Xue Li[3]; Feifei Tian[4]; Zhezhe Cui[5]; Wei Chen[2,3,#]

ABSTRACT

Introduction: Tuberculosis (TB) represents one of China's most significant infectious disease, with inter-provincial population migration posing a challenge to controlling its spread. This study examined TB cases among inter-provincial migrants across China from 2019 to 2023.

Methods: TB surveillance data were extracted from China's Tuberculosis Information Management System and analyzed using R software (version 4.4.0). After information desensitization, the relevant information of TB patients with differing current and permanent address codes was extracted.

Results: Between 2019 and 2023, we identified 123,945 TB cases among inter-provincial migrants, representing 4.03% (123,945/3,077,951) of all reported TB cases. The primary destination provincial-level administrative divisions (PLADs) for TB patients were Guangdong (48,183 cases, 38.9%), Zhejiang (27,383 cases, 22.1%), Fujian (8,582 cases, 6.9%), Beijing (7,959 cases, 6.4%), and Shanghai (7,403 cases, 5.9%), collectively accounting for 80.3% of all inter-provincial migrant TB cases. The PLADs with the highest outflow of TB migrants were Sichuan (15,155 cases, 12.23%), Hunan (14,707 cases, 11.87%), Guizhou (13,927 cases, 11.24%), Jiangxi (8,892 cases, 7.17%), and Hubei (8,441 cases, 6.81%). Among these migrant cases, 66.2% were male, 93.0% were newly diagnosed, 2.4% exhibited drug resistance. The proportion of individuals aged 45–64, aged ≥65 and re-treated exhibited a significant annual increase (P<0.001). The overall successful treatment rate was 89.5%, while 5.3% experienced adverse treatment outcomes. Throughout the study period, the lowest proportion of TB cases among inter-provincial migrants occurred in February.

Conclusion: From 2019 to 2023, the characteristics of TB among inter-PLADs migrant patients have undergone certain changes. The migration of TB primarily flows from economically weaker regions to more developed areas, with the main destination PLADs relatively stable. Effective TB control among inter-PLADs migrants requires targeted screening programs focusing on individuals from major source and destination PLADs. Tailored strategies should be developed based on the migration patterns of different PLADs.

Tuberculosis (TB) remains a significant global public health challenge. In 2022, approximately 10.6 million cases and 1.3 million deaths were reported worldwide (*1*). China has achieved substantial progress in reducing TB incidence, with a 3.1% annual decline between 2010 and 2022 (*2–3*). In 2022, the estimated number of new TB cases in China was 748,000 (*1*). However, a considerable gap persists between this progress and the World Health Organization (WHO)'s goal of ending TB by 2035. In 2023, the reported incidence rate of tuberculosis in China decreased to 43.49 per 100,000 people. However, significant disparities persist in reported incidence rates across different regions and populations, underscoring the need for targeted control measures tailored to specific areas and groups to enhance disease prevention effectiveness. Understanding the characteristics of diverse populations facilitates precise and localized interventions, with the migrant population emerging as a key demographic requiring focused attention. Many studies have demonstrated that human migration is an important factor that needs to be taken into consideration in the endeavor of preventing and controlling infectious diseases (*4*). Population mobility also has an impact on TB control (*4–5*).

In China, unbalanced economic development drives migration patterns, with individuals from less-developed regions commonly relocating to developed provincial-level administrative divisions (PLADs) seeking enhanced employment opportunities and higher incomes. According to the seventh National Population Census conducted by the National Bureau

of Statistics of China in 2020, China's population movement has become increasingly active, with the migrant population growth rate accelerating and approaching 380 million individuals (*6*). Multiple factors create substantial challenges for TB prevention and control among migrant populations. Migrant populations, particularly manual laborers whose living conditions and medical security are inferior to those of local workers, face circumstances that impede effective TB prevention and control. To enhance TB patient management within this demographic, the Chinese Anti-Tuberculosis Association issued the "Guidelines for the Management of Tuberculosis in Migrant Population" in 2021, emphasizing the critical importance of standardized TB management for this population (*7*).

Based on administrative divisions, the migrant population is categorized into intra-provincial and inter-provincial groups. Compared to intra-provincial migrants, inter-provincial migrants exhibit distinct characteristics (*8*–*9*). First, regarding the size of the floating population, recent trends in cross-provincial mobility have revealed new trends. Between 2007 and 2022, inter-provincial migration peaked in 2020 but demonstrated a sharp decline in subsequent years, with certain first-tier cities (e.g., Beijing) experiencing negative growth in their floating population sizes. Several provinces, including Henan, Jiangxi, and Hunan, exhibited net out-migration patterns in 2022, indicating regional shifts in migration attractiveness. Second, inter-provincial population movement primarily followed unidirectional inflow or outflow patterns, with relatively limited bidirectional interaction. This contrasts with the more cyclical or reciprocal movement patterns typically observed within provincial boundaries and suggests persistent pressures in inflow cities. Third, due to administrative divisions, service provision and management for inter-provincial floating populations face more complex challenges than those for intra-provincial mobility.This study focuses on epidemiological analysis of TB cases among inter-provincial migrants (TBIM) to provide evidence-based recommendations for improved prevention and control of TBIM.

METHODS

China's Tuberculosis Information Management System (TBIMS) is a web-based database launched in 2005, which encompasses all collected TB patients' basic information, diagnosis, treatment, management and outcome information and other related details. We extracted data on reported TB cases from 2019–2023 from the TBIMS, including both confirmed and clinically diagnosed cases across 31 PLADs in China. After removing personally identifiable information, we extracted relevant variables including sex, age, year of diagnosis, registration address, current address code, permanent address code, and treatment-related information. However, we excluded cases with extrapulmonary tuberculosis only, cases with diagnostic changes to other diseases, cases with virtual medical records, and cases with nontuberculous mycobacteria (NTM).

We defined inter-provincial migrants as individuals whose current address code differed from their permanent address code in the first two digits, which represent provincial administrative divisions. We analyzed the characteristics of inter-provincial migrants, including demographic features, inter-provincial mobility patterns, diagnostic classifications, treatment outcomes, and other epidemiological factors. We performed all data processing and statistical analyses using R software (version 4.4.0, Vienna, Austria) and Microsoft Excel 2021 (Redmond, USA). We described the data using rates and constituent ratios as appropriate. Trend statistical analysis was performed using the Cochran-Armitage trend test.

RESULTS

A total of 3,077,951 TB cases were reported from 2019 to 2023, of which 123,945 cases (4.03%) were inter-provincial migrants. TBMI cases decreased from 30,425 in 2019 to 19,801 in 2023. Among TBIM cases, males comprised 66.2% of the population. Individuals aged 15–44 years represented 65.6% of cases, constituting the predominant demographic group. The proportion of the 45–64 age group demonstrated a significant annual increase (Z=20.42, P<0.001), rising from 24.9% in 2019 to 32.6% in 2023, corresponding to an average annual growth rate of 6.9%. Similarly, the ≥65 age group exhibited a marked upward trend (Z=21.59, P<0.001), rising from 4.5% to 8.8% during the same period, reflecting an 18.25% average annual increase. The occupational distribution of inter-provincial TB migrants is presented in Table 1.

TABLE 1. Characteristics of inter-provincial migrants in China, 2019–2023.

Groups	2019 *n* (%)	2020 *n* (%)	2021 *n* (%)	2022 *n* (%)	2023 *n* (%)	Total *n* (%)
Sex						
Male	20,362 (66.9)	16,859 (65.7)	18,110 (65.8)	13,532 (65.9)	13,185 (66.6)	82,048 (66.2)
Female	10,063 (33.1)	8,814 (34.3)	9,406 (34.2)	6,998 (34.1)	6,616 (33.4)	41,897 (33.8)
Age (years)						
0–14	160 (0.5)	145 (0.6)	123 (0.4)	114 (0.6)	103 (0.5)	645 (0.5)
15–44	21,296 (70.0)	17,587 (68.5)	18,065 (65.7)	12,852 (62.6)	12,502 (58.1)	81,302 (65.6)
45–64	7,585 (24.9)	6,715 (26.2)	7,680 (27.9)	6,126 (29.8)	6,450 (32.6)	34,556 (27.9)
≥65	1,384 (4.5)	1,226 (4.8)	1,648 (6.0)	1,438 (7.0)	1,746 (8.8)	7,442 (6.0)
Occupations						
Children/students/teachers	1,605 (5.3)	1,251 (4.9)	1,309 (4.8)	902 (4.4)	834 (4.2)	5,901 (4.8)
Staff/workers	12,429 (40.9)	10,245 (39.9)	10,559 (38.4)	7,034 (34.3)	5,950 (30.0)	46,217 (37.3)
Farmers/herdsmen/fishermen/seafarers	4,762 (15.7)	3,926 (15.3)	3,856 (14.0)	3,299 (16.1)	3,568 (18.0)	19,411 (15.7)
Retired/housework/unemployed	9,811 (32.2)	8,885 (34.6)	10,464 (38.0)	8,167 (39.8)	8,222 (41.5)	45,549 (36.7)
Unknown and others	1,818 (6.0)	1,366 (5.3)	1,328 (4.8)	1,128 (5.5)	1,227 (6.2)	6,867 (5.5)

Among tuberculosis cases in inter-provincial migrants, the vast majority (93.0%) were newly treated patients. The proportion of re-treated cases showed a progressive annual rise (Z=7.48, P<0.001), increasing from 6.7% in 2019 to 8.2% in 2023. Laboratory confirmation was achieved in 70,858 cases (57.2%), while clinical diagnosis was established for 49,873 cases (40.2%). Cases lacking etiological evidence demonstrated a significant decreasing trend (Z=12.79, P<0.001), declining consistently over the study period. Drug susceptibility testing revealed that most patients (120,912 cases, 97.6%) harbored drug-susceptible strains, whereas 2.4% demonstrated drug resistance. Secondary tuberculosis represented the predominant disease classification (116,023 cases, 93.6%), with other forms comprising less than 7% of cases: primary tuberculosis (596 cases, 0.5%), hematogenous disseminated tuberculosis (580 cases, 0.5%), tracheobronchial tuberculosis (72 cases, 0.1%), and tuberculous pleurisy (5,845 cases, 4.7%). Treatment outcomes showed that 41.8% of inter-provincial tuberculosis migrants (51,812 cases) achieved cure, while 47.7% (59,166 cases) completed treatment successfully (Table 2).

From 2019 to 2023, Most PLADs exhibit unidirectional characteristics, primarily characterized by either outflow or inflow. Guangdong Province reported the highest number of TBIM cases among all PLADs, autonomous regions, and municipalities in China (Figure 1A). The distribution of TBIM cases demonstrated significant geographic concentration, with five PLADs accounting for the vast majority: Guangdong (48,183 cases, 38.9%), Zhejiang (27,383 cases, 22.1%), Fujian (8,582 cases, 6.9%), Beijing (7,959 cases, 6.4%), and Shanghai (7,403 cases, 5.9%). These five regions collectively represented 80.3% of all reported TBIM cases (Figure 1A). Conversely, the PLADs with the highest outflow of migrant TB cases included Sichuan (15,155 cases, 12.23%), Hunan (14,707 cases, 11.87%), and Guizhou (13,927 cases, 11.24%), Jiangxi (8,892 cases, 7.147%), and Hubei (8,441 cases, 6.81%) (Figure 1A). Some provinces, such as Qinghai, Xizang, and Ningxia exhibited relatively stable mobility patterns, with consistently minimal inflows and outflows.

Analysis of migration patterns revealed several critical relationships between major inflow and outflow PLADs, particularly involving Guangdong, Zhejiang, and Fujian as primary destinations; and Sichuan, Guizhou, and Hunan as major source regions. Among TBIM patients originating from Sichuan, 42.69% migrated to Guangdong, while approximately 49.82% of TBIM cases from Guizhou relocated to Zhejiang. The data further demonstrated that 77.13% of TBIM patients from Hunan chose Guangdong as their destination, and an overwhelming 88.69% of TBIM cases from Guangxi also migrated to Guangdong (Figure 1B).

Overall, the top five PLADs for TBMI inflow and outflow remained largely stable throughout the five-

TABLE 2. Diagnosis and treatment outcomes of TB among inter-provincial migrants in China, 2019–2023.

Type	2019 *n* (%)	2020 *n* (%)	2021 *n* (%)	2022 *n* (%)	2023 *n* (%)	Total *n* (%)
Treatment classification						
Newly treated	28,388 (93.3)	24,075 (93.8)	25,670 (93.3)	18,989 (92.5)	18,187 (91.8)	115,309 (93.0)
Re-treated	2,037 (6.7)	1,598 (6.2)	1,846 (6.7)	1,541 (7.5)	1,614 (8.2)	8,636 (7.0)
Bacteriological diagnosis						
Positive	15,181 (49.9)	13,906 (54.2)	15,830 (57.5)	12,692 (61.8)	13,249 (66.9)	70,858 (57.2)
Negative	14,138 (46.5)	11,150 (43.4)	11,028 (40.1)	7,318 (35.6)	6,239 (31.5)	49,873 (40.2)
Missing	1,106 (3.6)	617 (2.4)	658 (2.4)	520 (2.5)	313 (1.6)	3,214 (2.6)
Drug susceptibility						
Susceptible	29,683 (97.6)	24,995 (97.4)	26,862 (97.6)	20,052 (97.7)	19,320 (97.6)	120,912 (97.6)
Resistant	742 (2.4)	678 (2.6)	654 (2.4)	478 (2.3)	481 (2.4)	3,033 (2.4)
Classification of TB						
Primary TB	58 (0.2)	170 (0.7)	234 (0.9)	67 (0.3)	67 (0.3)	596 (0.5)
Hematogenous disseminated TB	127 (0.4)	125 (0.5)	122 (0.4)	104 (0.5)	105 (0.5)	580 (0.5)
Secondary TB	28,688 (94.3)	24,176 (94.2)	26,017 (94.6)	19,341 (94.2)	18,627 (94.1)	116,023 (93.6)
Tracheobronchial TB	0 (0)	1 (0.0)	1 (0.0)	37 (0.2)	33 (0.2)	72 (0.1)
Tuberculous pleurisy	1,552 (5.1)	1,201 (4.7)	1,142 (4.2)	981 (4.8)	969 (4.9)	5,845 (4.7)
Treatment outcomes						
Cured	11,725 (38.5)	10,728 (41.8)	12,292 (44.7)	9,607 (46.8)	Not available	44,352 (42.6)
Treatment completed	16,608 (54.6)	13,265 (51.7)	13,622 (49.5)	9,494 (46.2)		52,989 (50.9)
Adverse outcomes	1,640 (5.4)	1,379 (5.4)	1,365 (5.0)	1,165 (5.7)		5,549 (5.3)
Missing	452 (1.5)	301 (1.2)	237 (0.9)	264 (1.3)		1,254 (1.2)

Note: The above definition is sourced from the TBIMS system and aligns with the relevant definitions in the *Definitions and reporting framework for tuberculosis (2013 revision)*.
Not available: As the data collection period did not meet the required statistical timeframe for treatment outcomes in 2023, no statistical analysis was conducted.
Abbreviation: TB=tuberculosis.

year period, with notable exceptions observed in specific years: Guangxi (2020) and Anhui (2022) among outflow provinces, and Shandong (2020) among inflow provinces (Supplementary Figure S1, available at http://weekly.chinacdc.cn). TBMI populations from major outflow PLADs predominantly migrated to economically developed regions — primarily Guangdong, Zhejiang, Fujian, Shanghai, and Jiangsu — with migration flows extending to all 31 provinces (Supplementary Figure S2, available at http://weekly.chinacdc.cn).

From 2019 to 2023, tuberculosis cases among inter-provincial migrants were reported consistently throughout all months of the year. The proportion of monthly TBIM cases relative to the annual total demonstrated notable seasonal variation, reaching its lowest point in February. The proportion increased progressively from March through August before declining again, with February representing the nadir during the Chinese New Year period, recording 6,498 cases and accounting for 5.24% of the total (Figure 2). Comparing the data from February each year, the proportion of TBIM patients was lowest in February 2020 and highest in February 2023. The growth pattern of TBIM patients from January to March 2023 differed from that observed in other years.

DISCUSSION

China is a vast country with a large population and uneven economic development across regions. Additionally, people have the habit of returning to their hometowns or traveling during major holidays, all of which contribute to the high mobility of the population in China. This mobility facilitates disease transmission while intensifying demands for epidemic

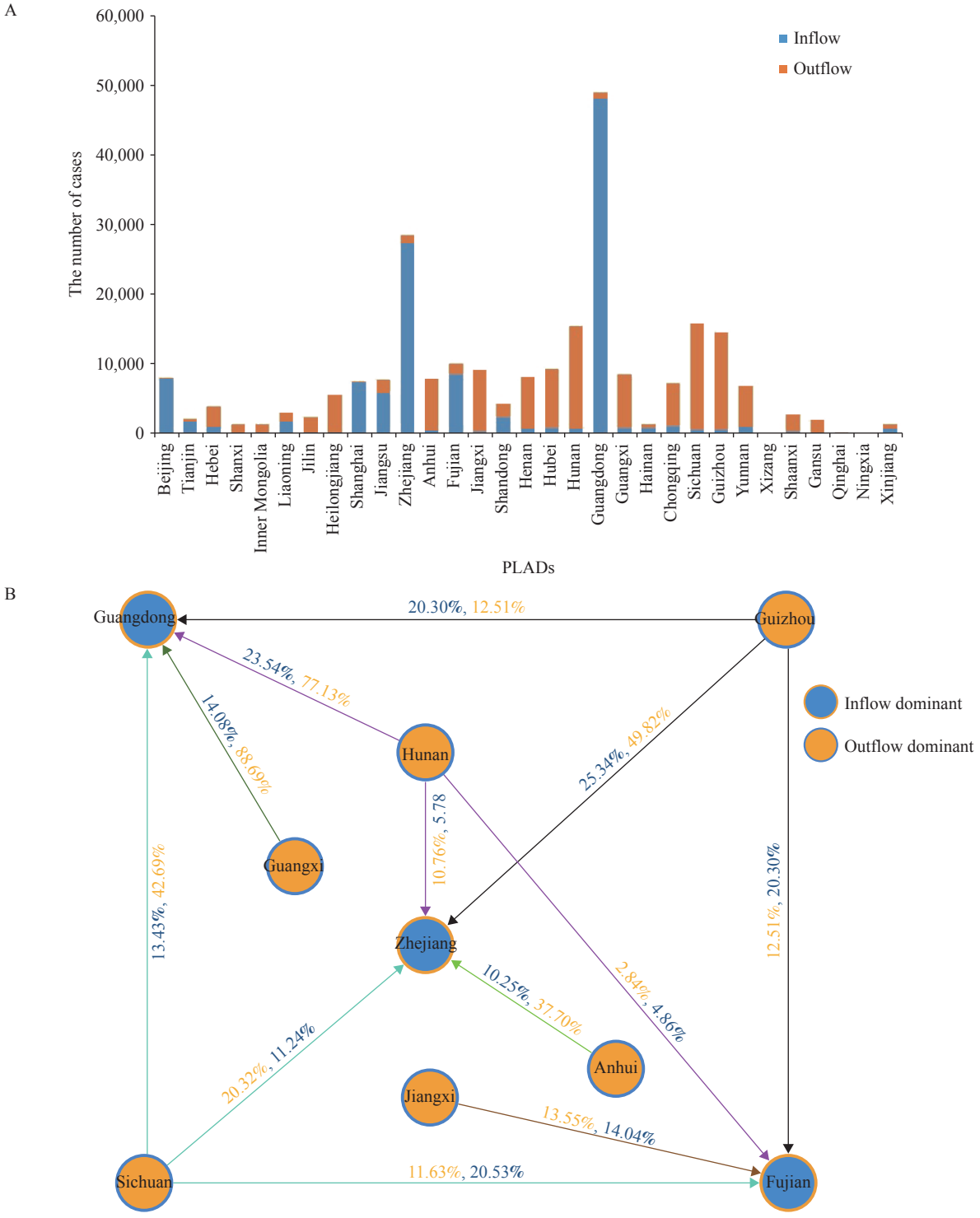

FIGURE 1. Flow patterns between PLADs for TBIM in China, 2019-2023. (A) The number of tuberculosis cases among inter-provincial migrants in China. (B) Key migration patterns between source and destination PLADs and the percentage of TB cases among inflow and outflow TB cases.
Abbreviation: PLADs=provincial-level administrative divisions; TB=tuberculosis; TBIM=TB cases amonginter-provincial migrants.

control — particularly for TB, which represents the third-highest global disease burden in China. Migrant populations also experience TB burden, with TB constituting the second most prevalent notifiable disease among interprovincial migrants during 2016–2020, characterized by elevated infection rates

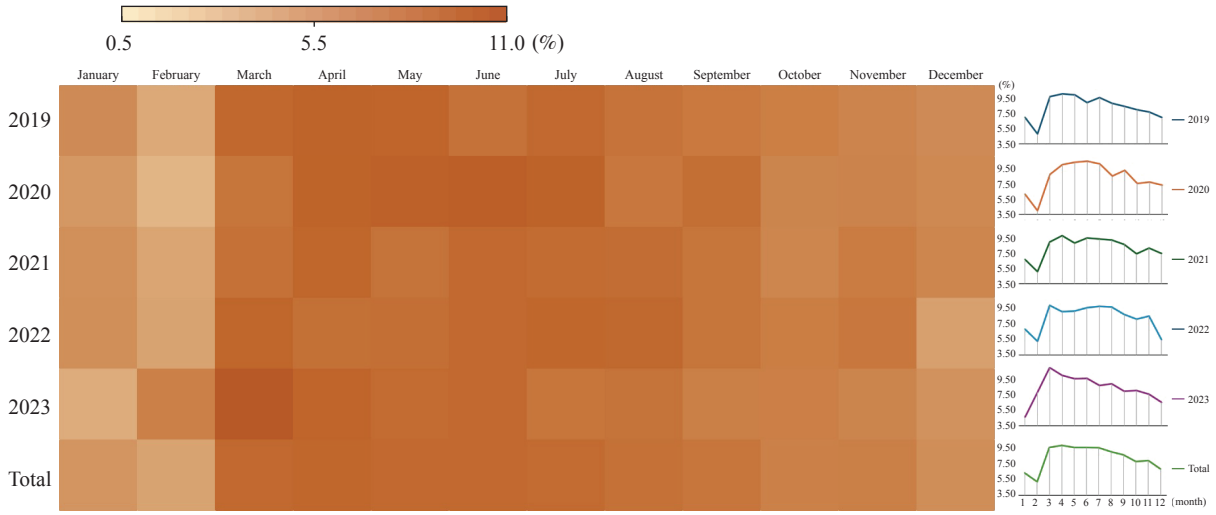

FIGURE 2. Monthly distribution of TBIM in China from 2019 to 2023.
Note: The monthly proportion of TBIM patients relative to the annual total was visualized through both a heat map and a line graph, stratified by year and month.

and extensive transmission scales (*4*). Our data indicate that inter-provincial migrants accounted for 4.03% of the total number of TB cases during the study period. TBIM were predominantly male (66.18%) and newly diagnosed (92.94%) TB cases. However, retreatment cases showed a significant upward trajectory (P<0.001). This may be related to their high mobility, which poses challenges such as treatment interruption, difficulty in tracking, and poor treatment adherence. Significant disparities exist between these migrants and local residents in terms of working and living environments, economic conditions, treatment adherence, and TB awareness (*10*–*11*). A study conducted in Kashgar Prefecture, Xinjiang Uygur Autonomous Region identified retreatment risk factors including low education level (primary school) [odds ratio (*OR*): 3.434, 95% confidence interval (*CI*): 1.861–6.337], BMI>24.00 (*OR*: 4.235, 95% *CI*: 1.277–7.877), non-standardized treatment (*OR*: 3.4346, 95% *CI*: 1.788–6.606), and smoking (*OR*: 3.970, 95% *CI*: 1.419–11.113)(*12*).

China's migrant population has expanded dramatically alongside economic and social development in recent years. Intra-provincial migration consistently exceeds inter-provincial movement, with the 2020 population census documenting 251 million intra-provincial migrants compared to 125 million inter-provincial migrants (*6*). Between 2019 and 2023, we identified 123,945 TB cases among the inter-provincial migrant population. Although intra-provincial migrants substantially outnumber inter-provincial migrants, the distribution of TB cases between these groups has shifted over time. Research conducted by Hu Dongmei and colleagues demonstrated that TB cases among the migrant population totaled 76,188, 70,749, and 42,628 in 2019, 2020, and 2021, respectively (*13*). When combined with our current findings, the proportion of inter-provincial migrant TB patients relative to all migrant TB patients remained below 40% in 2019 and 2020 but increased substantially to 64.5% in 2021.

Geographically, TB patients demonstrate uneven distribution patterns as migrant populations relocate from economically underdeveloped regions to more prosperous areas. Recent reports indicate that Guizhou, Sichuan, Jiangxi, and Hunan, characterized by weaker economies, exhibit higher TB incidence rates compared to economically advanced PLADs such as Guangdong, Zhejiang, and Fujian. The TB epidemiological characteristics (including incidence rates and disease burden) of the origin PLADs significantly influence TB occurrence among corresponding inter-provincial migrants (*14*). In Zhejiang, research demonstrated that TB cases among migrant populations comprised approximately one-third of all diagnosed cases during the study period (*15*). Effective control of inter-provincial TB patients remains essential for reducing overall disease burden. This study further revealed that most TB patients among migrant populations in Zhejiang originated from Guizhou, Anhui, and Zhejiang itself, findings that align with our research results.

Population mobility correlates strongly with economic dynamics. Specifically, lower economic development levels in outflow regions facilitate

population outflow, while higher economic development levels in inflow regions encourage population inflow. The economic disparity between regions is considered as a significant factor influencing population mobility (*16*). Existing research indicates that eastern provinces and municipalities such as Beijing, Shanghai, Guangdong, Zhejiang, Jiangsu, and Fujian are the primary inflow centers for migrant populations, though dispersion toward central and western regions has gradually increased (*16*). These findings align with the TBIM mobility patterns observed in this study, wherein TBIM outflow provinces tend to be economically weaker, while inflow provinces are predominantly more developed. This suggests that TBIM mobility may also be economically driven. However, other potential factors (e.g., education access, healthcare quality, outbreaks or control of other infectious diseases) warrant further investigation.

Several limitations constrained this study. First, our definition of the migrant population relied solely on address codes without incorporating migration duration or additional demographic factors. Second, we did not analyze TB incidence rates specifically within the inter-provincial migrant population. Furthermore, limited research has been conducted on the disease management status and migration-related factors affecting this population.

The defining feature of TBIM is high mobility, requiring location-specific disease control strategies. Disease control and health education can be implemented through "point-to-point" initiatives in high-volume inflow/outflow provinces or cities. Particular attention should be paid to subgroups that have shown a significant growth trends, such as people ≥45 years old. Research indicates that interventions, such as providing transportation and nutritional support, and expanded outpatient services can improve treatment success and reduce TB incidence in migrant populations(*15*).

Conflicts of interest: No conflicts of interest.

Acknowledgements: Ms. Minying Huang (Guangxi CDC), Ms. Xiaoyan Liang (Guangxi CDC), and Dr. Zhijun Li (U.S. CDC China Office) for their valuable contributions to this investigation.

Funding: Supported by the Central Finance Tuberculosis Project (2528) and the Project of National Key Laboratory of Intelligent Tracking and Forecasting for Infectious Diseases (202303).

doi: 10.46234/ccdcw2025.180

[#] Corresponding author: Wei Chen, chenwei@chinacdc.cn.

[1] National Institute for Communicable Disease Control and Prevention, Chinese Center for Disease Control and Prevention, Beijing, China; [2] Chinese Field Epidemiology Training Program, Chinese Centre for Disease Control and Prevention, Beijing, China; [3] National Center for Tuberculosis Control and Prevention, Chinese Centre for Disease Control and Prevention, Beijing, China; [4] Daxing Center for Disease Control and Prevention, Beijing, China; [5] Guangxi Zhuang Autonomous Region Center for Disease Control and Prevention, Nanning City, Guangxi Zhuang Autonomous Region, China.

Submitted: May 22, 2025
Accepted: August 11, 2025
Issued: August 15, 2025

REFERENCES

1. World Health Organization. Global tuberculosis report 2023. Global report. Geneva: World Health Organization; 2023. https://www.who.int/publications/i/item/9789240083851.
2. Wang XY, Jiang ML, Pang YJ, Sun DJY, Yu CQ, Wang L, et al. Current status of tuberculosis burden in China. Chin J Epidemiol 2024;45(6):857 – 64. https://doi.org/10.3760/cma.j.cn112338-20240311-00111.
3. Xu CH, Zhao YL. Commit, invest and deliver: towards achieving end tuberculosis strategy goals through active case finding and preventive treatment in China. China CDC Wkly 2025;7(13):407 – 12. https://doi.org/10.46234/ccdcw2025.068.
4. Yu LJ, Ji PS, Ren X, Wang YH, Lv CL, Geng MJ, et al. Inter-city movement pattern of notifiable infectious diseases in China: a social network analysis. Lancet Reg Health West Pac 2025;54:101261. https://doi.org/10.1016/j.lanwpc.2024.101261.
5. Li M, Quan Z, Xu P, Takiff H, Gao Q. Internal migrants as drivers of long-distance cross-regional transmission of tuberculosis in China. Clin Microbiol Infect 2025;31(1):71 – 7. https://doi.org/10.1016/j.cmi.2024.09.005.
6. Hou JW. New characteristics and trends of population development in China: an analysis based on seven Chinese censuses. Acad Forum 2021;44(5):1 – 14. https://doi.org/10.16524/j.45-1002.2021.05.012.
7. Chinese Antituberculosis Association. Guidelines for the management of tuberculosis patients in floating population. Electron J Emerg Infect Dis 2021;6(1):7 – 12. https://doi.org/10.19871/j.cnki.xfcrbzz.2021.01.002.
8. Zeng WQ. Research on the spatial spillover effect of local fiscal expenditure on inter-provincial population mobility [dissertation]. Nanchang, China: Jiangxi University of Finance and Economics; 2024. http://dx.doi.org/10.27175/d.cnki.gjxcu.2024.000202. (In Chinese).
9. Subinur. A study on the characteristics and changing trends of inter-provincial population mobility in China: a spatial econometric analysis based on 2000—2020 population census data [dissertation]. Harbin, China: Harbin Engineering University; 2023. http://dx.doi.org/10.27060/d.cnki.ghbcu.2023.000495. (In Chinese).
10. Tang Y, Zhao MG, Wang YX, Gong YH, Yin X, Zhao AG, et al. Non-adherence to anti-tuberculosis treatment among internal migrants with pulmonary tuberculosis in Shenzhen, China: a cross-sectional study. BMC Public Health 2015;15:474. https://doi.org/10.1186/s12889-015-1789-z.
11. Zou X, Zhou L, Wu HZ, Chen L, Zhou FJ, Gong C, et al. The role of tuberculosis control institutes in delivering tuberculosis information to domestic migrants in China: a multi-level analysis of a nationwide cross-sectional survey. Int J Infect Dis 2019;86:94 – 101. https://doi.org/10.

1016/j.ijid.2019.06.021.
12. Abulimit M, Tusun D, Wubulikasimu K, Aihaiti M, Liu ZJ, Li B, et al. Analysis of influencing factors of recurrence after successful treatment in new pulmonary tuberculosis patients in Kashgar Prefecture, Xinjiang Uygur Autonomous Region. Chin J Antituberc 2022;44(11):1148 – 53. https://doi.org/10.19982/j.issn.1000-6621.20220299.
13. Hu DM, Xu CH, Zhao YL. Analysis on the epidemiological characteristics of pulmonary tuberculosis among floating population in China from 2018 to 2021. J Trop Dis Parasitol 2023;21(2):78 – 81, 107. https://doi.org/10.3969/j.issn.1672-2302.2023.02.004.
14. Lin HH, Zhang R, Wu ZY, Li MJ, Wu JM, Shen X, et al. Assessing the spatial heterogeneity of tuberculosis in a population with internal migration in China: a retrospective population-based study. Front Public Health 2023;11:1155146. https://doi.org/10.3389/fpubh.2023.1155146.
15. Liu K, Chen SH, Zhang Y, Li T, Xie B, Wang W, et al. Tuberculosis burden caused by migrant population in Eastern China: evidence from notification records in Zhejiang Province during 2013-2017. BMC Infect Dis 2022;22(1):109. https://doi.org/10.1186/s12879-022-07071-5.
16. Ke WQ, Xiao BY, Lin LY, Zhu Y, Wang Y. Interprovincial urban and rural floating population evolution of China and its relationship with regional economic development. Acta Geogr Sin 2023;78(8):2041 – 57. https://doi.org/10.11821/dlxb202308012.

SUPPLEMENTARY MATERIAL

C

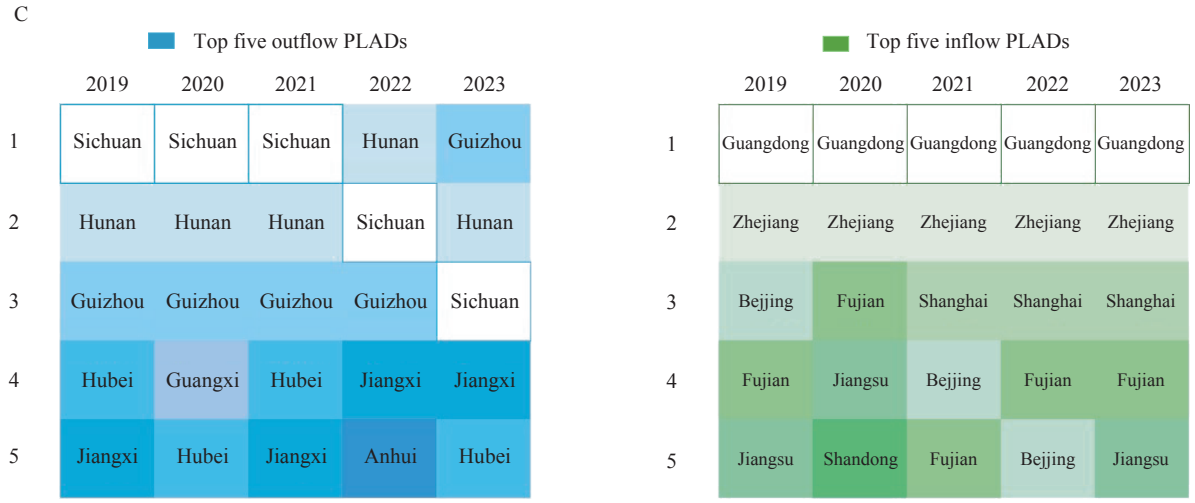

SUPPLEMENTARY FIGURE S1. The top five outflow or inflow PLADs, 2019–2023.
Abbreviation: PLAD=provincial-level administrative division.

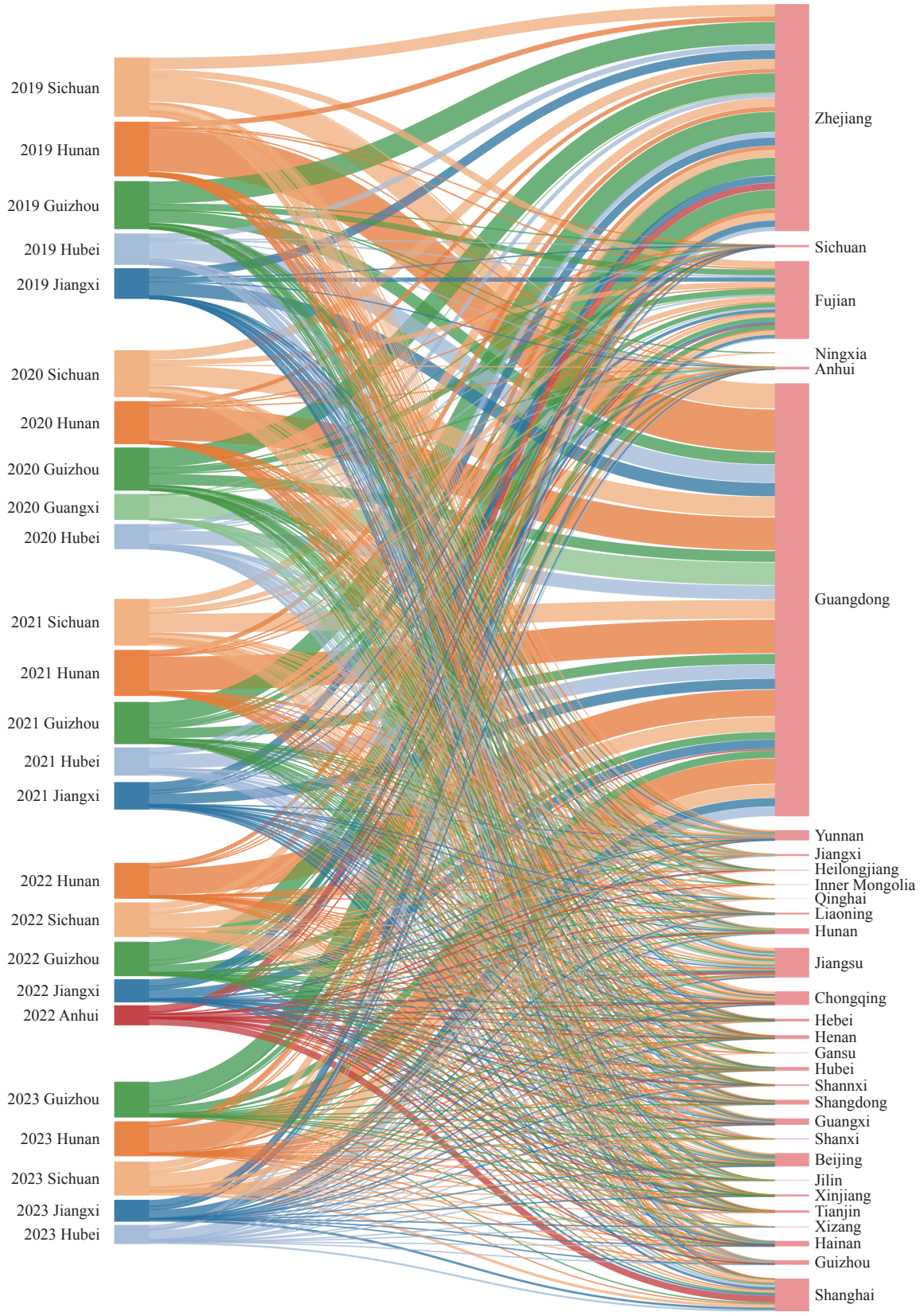

SUPPLEMENTARY FIGURE S2. Migration patterns of TBIM patients from the top five out-migration provinces, 2019–2023. Note: The length of the colored blocks is proportional to the number of migrants, and the lines indicate the direction of migration.

Outbreak Reports

An Outbreak of Isoniazid-Resistant Tuberculosis in a School Originating from Household Transmission — Guigang City, Guangxi Zhuang Autonomous Region, China, November 2024

Da Xu[1,2,3,&]; Xiaoyan Liang[1,&]; Lingyun Zhou[1,&]; Wei Chen[3,4]; Jing Ye[1]; Juan Li[1]; Weihua Yao[5]; Jinhui Zhu[6,#]; Zhezhe Cui[1,#]

Summary

What is already known about this topic?

Tuberculosis (TB) represents one of the world's most significant infectious diseases, caused by *Mycobacterium tuberculosis* (*M. tuberculosis*). The pathogen spreads readily among students due to crowded environments and prolonged close contact during school activities.

What is added by this report?

This outbreak investigation identified 18 TB cases (15 students, 1 teacher, and 2 staff members), including 5 cases with isoniazid-resistant TB. Sixteen pulmonary TB cases demonstrated clear epidemiological linkage, indicating a clustered outbreak spanning multiple households, school grades, and both junior and senior high schools.

What are the implications for public health practice?

This outbreak underscores the critical importance of comprehensive household contact screening. When tuberculosis emerges within a family unit, school contacts — particularly students and teachers — require immediate and thorough screening. Additionally, the outbreak reveals significant gaps in the effectiveness and quality of entrance physical examinations that demand urgent improvement.

ABSTRACT

Introduction: On November 27, 2024, an active pulmonary tuberculosis case (pathogen positive) was identified in a senior high school in Guigang City, Guangxi Zhuang Autonomous Region, China.

Methods: A comprehensive field epidemiological investigation was conducted to identify close contacts. Close contacts underwent detailed interviews regarding their exposure history and symptoms, followed by diagnostic testing including the recombinant *M. tuberculosis* fusion protein test or interferon-γ release assay, along with chest X-ray or CT imaging. Suspected cases were subjected to comprehensive laboratory evaluation, including sputum smear microscopy, sputum culture, and molecular biological testing. Drug susceptibility testing and genomic sequencing analysis were performed on culture-positive strains. Epidemiological associations were systematically assessed.

Results: Screening encompassed 957 close contacts (919 from the senior high school and 38 from the index case's junior high school class). Among these contacts, 18 active pulmonary tuberculosis cases (16 epidemiologically linked and 2 sporadic), 12 suspected cases, and 36 latent tuberculosis infections were identified. Four *M. tuberculosis* strains were successfully isolated from epidemiologically associated cases (including the index case, his junior high school classmate, high school deskmate, and current teacher). Genomic sequencing revealed that all strains exhibited isoniazid resistance and demonstrated high genetic homology (with <6 single nucleotide polymorphisms, SNPs). The index case had exhibited symptoms including cough and expectoration during junior high school; however, no abnormalities were detected during the physical examination upon senior high school enrollment. Additionally, routine daily health screenings conducted during morning and afternoon periods yielded consistently normal results. The investigation revealed that the index case had significant family contact history, with his father, two uncles, grandfather, and grandmother diagnosed with active pulmonary tuberculosis between 2019 and 2025, three of whom had confirmed isoniazid-resistant tuberculosis.

Conclusion: This outbreak represented a tuberculosis cluster resulting from household transmission that subsequently spread across different

school grades and classes. The delayed identification of the index case, attributable to multiple systemic factors, constituted the primary driver of disease dissemination. These findings underscore the critical importance of screening close contacts, particularly those who are teachers or students within affected families.

On November 27, 2024, the Qintang CDC in Guigang City of Guangxi Zhuang Autonomous Region received notification from Guigang CDC regarding a severe student pulmonary tuberculosis (PTB) case at a local high school. Preliminary screening conducted by Qintang CDC revealed 26 cases (47.27%) with strongly positive EC (Recombinant Mycobacterium Tuberculosis Fusion Protein) skin test results and 4 cases (7.27%) with abnormal chest X-ray findings. Subsequently, Guangxi Zhuang Autonomous Region (Guangxi) CDC, Guangxi Chest Hospital, and Guangxi Health Supervision Institute launched a joint investigation. Comprehensive screening of 957 close contacts — including 919 individuals from the senior high school and 38 from the junior high school — identified 18 active TB cases, 12 suspected TB cases, and 36 latent TB infections (LTBI). By the conclusion of the previous semester, a total of 22 tuberculosis cases had been confirmed: three cases were reclassified from "suspected" status following additional diagnostic workup, and one case progressed from latent TB infection to active disease. This outbreak, originating from household transmission, spread across both junior and senior high school populations. This report presents the epidemiological investigation and laboratory analysis of this outbreak to inform management strategies for similar future incidents.

INVESTIGATION AND RESULTS

Description of Index Case and Epidemiological Investigation

The outbreak occurred at a boarding high school comprising 51 classes across three grade levels, with a total enrollment of 2,699 students and 215 staff members. Each classroom occupied approximately 64 m^2 and accommodated around 55 students, featuring adequate natural ventilation and maintained cleanliness standards. Student dormitories (approximately 24 m^2 each) housed 14 residents and were equipped with two electric fans and one air conditioning unit. Each dormitory provided cross-ventilation through doors and windows positioned at opposite ends. Male dormitories lacked private bathrooms, while female dormitories included individual bathroom facilities.

The index case was a 16-year-old underweight male freshman who had experienced chronic productive cough during his junior high school enrollment (Class 55), though this condition received inadequate clinical attention at that time. During the investigation period, he was enrolled as a student in Class 2403 of the senior high school and resided in Dormitory 311. In September 2024, he completed the mandatory freshman entrance physical examination, during which the tuberculin skin test (TST) yielded negative results. On October 17, 2024, he presented to the local community health center with a 3-day history of cough and sputum production. Physical examination revealed bilateral coarse crackles; however, chest radiography was not performed. Daily health screening records maintained by his class documented no abnormal findings from September 1, 2024, through the day preceding symptom onset.

On November 14, 2024, the patient presented to Gangbei District People's Hospital of Guigang City with a two-month history of recurrent productive cough and fever. Due to disease severity, he was subsequently transferred to Guigang People's Hospital and then to Nanning Fourth People's Hospital. Initial evaluations indicated that surgical intervention might be necessary. On November 30, 2024, revised diagnostic imaging revealed secondary pulmonary TB with bilateral involvement: cavitary lesions in the right upper and middle lobes and left upper lobe (newly diagnosed, smear-positive), left-sided tuberculous pleurisy (newly diagnosed, smear-negative), complicated by left hydropneumothorax with approximately 80% compression of left lung parenchyma. Drug-susceptibility testing results provided on December 12, 2024, indicated rifampicin sensitivity but isoniazid resistance (Hr)-TB.

Following the *Guidelines for Tuberculosis Prevention and Control in Chinese Schools (2020)*, Qintang CDC initiated comprehensive case investigation and close contact screening. The investigation revealed that the index case had exhibited prolonged symptoms of cough and sputum production during junior high school, which had not received adequate medical attention. Notably, the index case had a significant family history of TB. His father received an active PTB

diagnosis in 2019, followed by his grandfather (2021), two uncles (2021), and grandmother (2025). Among these family members, the father, grandfather, and one uncle were Hr-TB cases (Figure 1).

Expanded Screening

Three rounds of close contact screening were conducted (Table 1). The first-round screening (November 29–December 3, 2024) targeted 66 individuals comprising 52 students and 14 teachers from the index case's class. The second-round screening (December 3–December 8, 2024) encompassed 405 individuals including 367 students and 38 teachers from adjacent floors and classes. The third-round screening (December 9–December 12, 2024) involved 448 individuals, including contacts from classes taught by the case teacher, the index case's junior high school classmate Li xx's class, and dormitory contacts. Screening for class 55 (the class where the index case studied during junior high school) was conducted from December 7th to 20th, 2024. All screening protocols included recombinant *M. tuberculosis* fusion protein skin test and chest digital radiography (DR), with selected participants undergoing interferon-γ release assay (IGRA) testing and computed tomography (CT) scanning. The first round identified 22 positive individuals (22/66) on skin testing, four with abnormal DR findings (4/66), leading to the detection of four confirmed cases and 17 suspected cases. The second round identified 12 positive individuals (12/405) on skin testing, with no abnormal DR findings; CT re-examinations of these 12 individuals revealed one new clinically diagnosed case and one suspected case. The third round identified nine positive individuals (9/448) on skin testing and one with abnormal DR findings (1/448); CT re-examinations of ten individuals detected two new clinically diagnosed cases (a school security guard and a canteen staff member, with no epidemiological links to the previous cases) and four suspected cases (two students, one canteen staff member, and one convenience-store employee). Concurrent screening of close contacts from the index case's former junior high school class identified three additional active PTB cases, including Li xx (who studied at the same senior high school as the index case but in a different class, and was confirmed as a PTB case on December 8th), Qin xx, and Wang xx (Figure 1). Following final confirmation by the Guangxi Chest Hospital, a total of 18 confirmed TB cases were identified, including one index case, seven confirmed cases (as referenced earlier), and ten additional cases reclassified from suspected to confirmed status (Table 1). Furthermore, 12 patients were categorized as suspected TB cases.

Outbreak Control and Treatment Outcomes

Following the tuberculosis outbreak, relevant agencies launched a coordinated response. The school conducted comprehensive contact tracing and screening of staff and students while implementing tuberculosis prevention education campaigns. Daily health monitoring was intensified, sick-leave data were systematically tracked, and targeted psychological

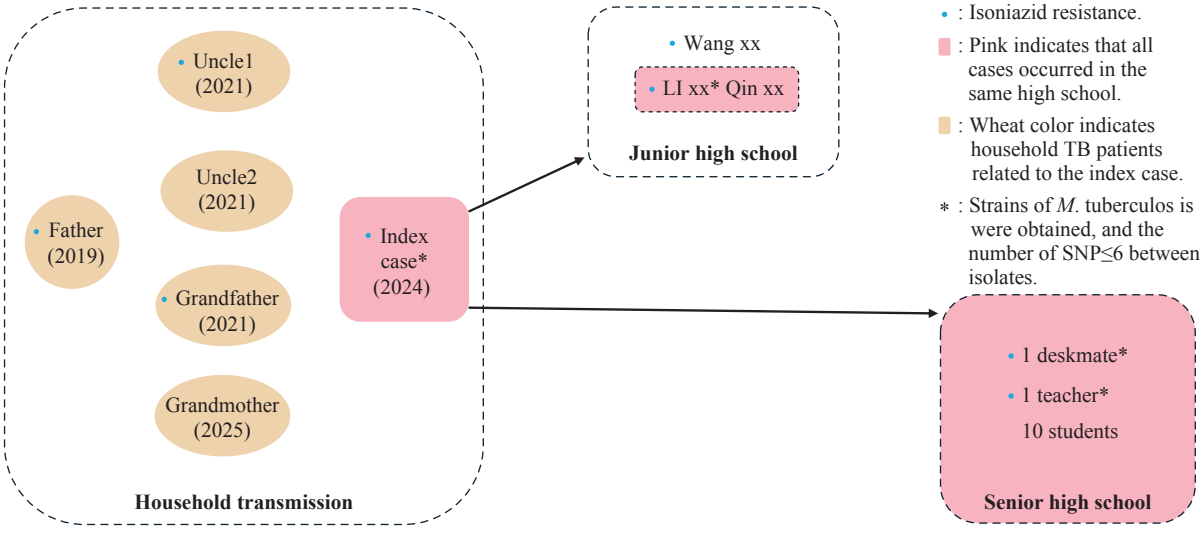

FIGURE 1. The transmission between household and school.
Abbreviation: TB=tuberculosis.

TABLE 1. The details of close contacts screening.

Screening	Class number and location	Duration	Number of screened cases	Number of newly confirmed cases	Number of newly suspected cases
First-round screening	2403: the index case's class.	11.29–12.3	66	11: four confirmed cases and 7 reclassified from suspected to confirmed status, 1 teacher and 10 students.	8
Second-round screening	2401, 2402, 2404 and 2405: The same floor; 2316: Up floor; 2406, 2407, 2408, 2409 and 2410: classes of students residing on the same dormitory floor.	12.3–12.8	405	1	1
Third-round screening	2419: Li xx's (the index case's junior high school classmate) class; 2413: Qin xx's (the index case's junior high school classmate) class; 2416, 2417 and 2418: the classes of students residing on the same dormitory floor; 2407, 2409 and 2412: the class taught by the teacher.	12.9–12.12	448	2: 2 staff.	3
Other	55: the Junior high school where the index case once studied.	12.7–12.20	38	3: Li xx, Qin xx and Wang xx (the index case's junior high school classmates)	0

support was provided to students, parents, and staff to address concerns and alleviate fears. The CDC provided technical guidance on screening protocols and containment measures, conducted thorough epidemiological investigations, assisted in identifying close contacts, disseminated evidence-based preventive strategies, and maintained timely communication with all stakeholders regarding outbreak developments. The hospital managed diagnosis, treatment, and follow-up care, and issued medical clearance documentation for safe return to school or work.

Upon comprehensive review and expert panel consultation, 15 students, one teacher, and two other staff members were confirmed as having pulmonary tuberculosis, along with 48 suspected and latent infection cases. Among confirmed cases, six were etiologically positive. All confirmed pulmonary tuberculosis cases received either home isolation treatment or hospitalization based on clinical severity. Of the suspected and latent tuberculosis infection cases, two required hospitalization (meeting established hospitalization criteria) and 16 received preventive treatment. By the end of the previous semester, three cases had transitioned from suspected to confirmed tuberculosis patients, one case had progressed from latent infection undergoing preventive treatment to active tuberculosis, and the remaining cases continued under follow-up monitoring or preventive treatment protocols. The confirmed patients were distributed across classes 2403, 2402, 2413, and 2419, involving boys' dormitories 311, 312, and 406, as well as girls' dormitories 408, 406, and 509. Four strains of *M. tuberculosis* were successfully isolated during this outbreak, including strains from the index patient and epidemiologically linked cases from junior high school. Drug susceptibility testing revealed that all four isolates demonstrated isoniazid resistance. Whole-genome sequencing demonstrated ≤6 single nucleotide polymorphisms (SNPs) between isolates, and genotype analysis confirmed that all strains belonged to the Beijing genotype.

DISCUSSION

Tuberculosis control in schools represents a critical public health priority in China; however, outbreaks continue to pose significant challenges. From 2008 to 2018, the reported incidence rate of TB among students was approximately one-third to one-fourth that of the general population, exhibiting an initial decline followed by an upward trend (*1*). The rate declined from 27.92 per 100,000 population in 2008 to 13.30 per 100,000 in 2015, then gradually increased to 17.97 per 100,000 in 2018 (*1*). The reported TB incidence among students was highest in the western region and lowest in the eastern region (*2*). The outbreak described in this study occurred in Guangxi, a province in southwest China with a reported TB incidence rate of 67.54 per 100,000 in 2023.

Tuberculosis outbreaks typically occur among individuals living in close-contact environments, with schools being common sites of transmission. Outbreaks usually occur within the same class or dormitory.

However, this outbreak exhibited distinct epidemiological characteristics and demonstrated high clustering patterns. With the exception of two staff members, all PTB cases were epidemiologically linked, indicating that this represented a cross-household, cross-school-grade, cross-junior/senior-high-school clustered outbreak. In this outbreak, five cases were Hr-TB. Although the management of isoniazid-resistant tuberculosis and drug-sensitive tuberculosis during an outbreak follows similar protocols, their treatment regimens and public health implications differ substantially. Compared with drug-sensitive tuberculosis patients, patients with Hr-TB demonstrate higher treatment failure rates (11% *vs.* 1%), higher recurrence rates (10% *vs.* 5%), and higher rates of acquired resistance (8% *vs.* 0.3%) (*3*). Molecular epidemiological studies have been widely utilized in contact tracing to understand person-to-person transmission patterns. Spacer oligonucleotide typing (spoligotyping) and MIRU-VNTR typing (mycobacterial interspersed repetitive units-variable number of tandem repeats) are commonly employed typing methods, but they are unsuitable for confirming transmission events in China, due to their limited ability to identify transmission chains in most TB outbreak scenarios. Several studies have demonstrated the utility of whole-genome sequencing (WGS) in epidemiological investigations and have suggested that WGS offers superior discriminatory power compared to spoligotyping and VNTR typing (*4*–*6*). In this outbreak, we employed WGS in our epidemiological investigation and demonstrated extremely high genetic similarity (<6 SNPs) between isolates. These results provided evidence that transmission may have begun during junior high school and originated from a single recent transmission source. However, it remains impossible to accurately determine the onset time of the identified cases, and thus the exact transmission chain cannot be definitively established. Based on epidemiological associations and the WGS results, we conclude that the primary transmission chain of this outbreak most likely originated within a household and subsequently spread from the index case to close contacts, including classmates, roommates, and the teacher. The remaining two cases, involving school staff, showed no obvious epidemiological links with the aforementioned 16 cases and may represent independent infections from other sources. As no bacterial isolates were obtained from these cases, further molecular analysis was not possible.

LTBI represents a persistent immune response to *M. tuberculosis* infection without clinical manifestations or radiological evidence of active disease (*7*). Approximately 23% of the global population harbors LTBI. Among infected individuals, 5% to 10% will progress to active tuberculosis during their lifetime. Given the substantial prevalence of LTBI, even a modest progression rate to active disease could significantly impact tuberculosis control efforts. Consequently, preventive treatment was administered to selected cases in this outbreak.

The fusion protein skin test or tuberculin skin test serves as a standard screening method; however, false-negative results may occur in certain cases. This limitation may have contributed to the failure to detect the index patient during school enrollment screening. Furthermore, multiple additional factors likely contributed to this public health emergency. First, the diagnosis of the index case experienced significant delay. Second, daily symptom monitoring and student absenteeism tracking failed to identify symptomatic students. This outbreak underscores the critical importance of household contact screening, particularly when household members include students or teachers. Simultaneously, the outbreak has highlighted the need to enhance the quality and effectiveness of freshman entrance physical examinations. Essential routine practices such as monitoring and documenting illness-related absenteeism, conducting daily morning and afternoon health screenings, and providing comprehensive health education require strengthening and standardization.

Conflicts of interest: No conflicts of interest.

Acknowledgements: Mr. Canyou Zhang (China CDC), Ms. Hui Chen (China CDC), Ms. Shan Yu (Chinese PLA General Hospital), and Dr. Zhijun Li (U.S. CDC China Office) for their valuable contributions to this investigation.

Funding: Supported by the National Key R&D Program of China (2022YFC2305204) and the Guangxi Medical and Health Key Discipline Construction Project (2022-06-21).

doi: 10.46234/ccdcw2025.183

[#] Corresponding authors: Zhezhe Cui, gxcdctbi@wsjkw.gxzf.gov.cn; Jinhui Zhu, cdc@wsjkw.gxzf.gov.cn.

[1] Institute of Tuberculosis Control and Prevention, Guangxi Zhuang Autonomous Region Center for Disease Control and Prevention, Nanning City, Guangxi Zhuang Autonomous Region, China; [2] National Institute for Communicable Disease Control and Prevention, Chinese Center for Disease Control and Prevention, Beijing, China; [3] Chinese Field Epidemiology Training Program, Chinese Centre for Disease Control and Prevention, Beijing, China;

[4] National Center for Tuberculosis Control and Prevention, Chinese Centre for Disease Control and Prevention, Beijing, China; [5] Guigang City Center for Disease Control and Prevention, Guigang City, Guangxi Zhuang Autonomous Region, China; [6] Guangxi Key Laboratory of Major Infectious Disease Prevention and Control and Biosafety Emergency Response, Guangxi Zhuang Autonomous Region Center for Disease Control and Prevention, Nanning City, Guangxi Zhuang Autonomous Region, China.
[&] Joint first authors.

Submitted: May 08, 2025
Accepted: August 08, 2025
Issued: August 15, 2025

REFERENCES

1. Cheng J, Liu JJ. Current status and progress of surveillance and automated-alert for tuberculosis in school. Chin J Antituberc 2020;42(5):436 – 41. https://doi.org/10.3969/j.issn.1000-6621.2020.05.005.
2. Chen H, Xia YY, Zhang CY, Cheng J, Zhang H. Epidemic trends and characteristics of pulmonary tuberculosis in students in China from 2014 to 2018. Chin J Antituberc 2019;41(6):662 – 8. https://doi.org/10.3969/j.issn.1000-6621.2019.06.013.
3. Gegia M, Winters N, Benedetti A, van Soolingen D, Menzies D. Treatment of isoniazid-resistant tuberculosis with first-line drugs: a systematic review and meta-analysis. Lancet Infect Dis 2017;17(2):223 – 34. https://doi.org/10.1016/S1473-3099(16)30407-8.
4. Nikolayevskyy V, Niemann S, Anthony R, van Soolingen D, Tagliani E, Ködmön C, et al. Role and value of whole genome sequencing in studying tuberculosis transmission. Clin Microbiol Infect 2019;25(11):1377 – 82. https://doi.org/10.1016/j.cmi.2019.03.022.
5. Yin XW, Zhang Q, Wang YT, Tao BL, Zhang XL, Shi JY, et al. Genomic and spatial analysis on the recent transmission of *Mycobacterium tuberculosis* in eastern China: a 10-year retrospective population-based study. Infect Drug Resist 2024;17:4257 – 69. https://doi.org/10.2147/IDR.S480621.
6. Nikolayevskyy V, Kranzer K, Niemann S, Drobniewski F. Whole genome sequencing of *Mycobacterium tuberculosis* for detection of recent transmission and tracing outbreaks: a systematic review. Tuberculosis 2016;98:77 – 85. https://doi.org/10.1016/j.tube.2016.02.009.
7. WHO. Guidelines Approved by the Guidelines Review Committee. Latent tuberculosis infection: updated and consolidated guidelines for programmatic management. Geneva: World Health Organization, 2018. https://www.who.int/publications/i/item/9789241550239.

Outbreak Reports

A Foodborne Outbreak Associated with ST59-*spa* t441-SCC*mec* IVa Methicillin-resistant *Staphylococcus aureus* Producing Enterotoxins A and B — Puyang City, Henan Province, China, September 2024

Zhijie Zhao[1,&]; Xiaoyue Wei[2,&]; Aimei Wang[1]; Wanting Wang[2]; Xiaofei Meng[1]; Wentao Liu[2]; Yanlin Chang[1]; Yakun Zhao[2]; Guangkang Li[1]; Jianling Chen[2]; Yongli Li[3]; Yuanhai You[2]; Ling Zhao[1]; Jianzhong Zhang[2]; Xianying Yan[1]; Zhigang Cui[2]; Guofeng Xu[1]; Haijian Zhou[2]; Xiaomei Yan[2,#]; Qingjie Zhang[1,#]

Summary

What is already known about this topic?

Staphylococcus aureus (*S. aureus*) represents a clinically significant pathogen and serves as a common causative agent of foodborne intoxication. The *S. aureus* strain ST59 constitutes the predominant clone associated with both community-associated methicillin-resistant *S. aureus* (CA-MRSA) and hospital-associated MRSA (HA-MRSA) infections. However, staphylococcal food poisoning (SFP) outbreaks attributed to ST59 MRSA have been documented in only a limited number of Chinese cities through retrospective investigations.

What is added by this report?

This report documents the first recorded outbreak of staphylococcal food poisoning (SFP) in Henan Province, which was attributed to the ST59-*spa* t441-SCC*mec* IVa CA-MRSA strain producing enterotoxins A and B. The confirmed source of the outbreak was contamination of donkey and goose meat with *S. aureus* enterotoxins A and B. Additionally, comprehensive genomic analysis identified multiple virulence genes and antibiotic resistance genes within the outbreak-related strains.

What are the implications for public health practice?

The identification of foodborne clones of ST59 CA-MRSA in this outbreak underscores the prevalence and transmission risks associated with this hypervirulent lineage. These findings highlight the critical need to strengthen surveillance measures for CA-MRSA among food industry workers and implement enhanced food safety protocols.

ABSTRACT

Introduction: On September 16, 2024, the Puyang City CDC received a report of a suspected foodborne disease outbreak involving 14 individuals who developed nausea, vomiting, and diarrhea following attendance at a hotel banquet. Upon notification, the District CDC immediately deployed a specialized investigation team to characterize the epidemiological features of the outbreak, identify the causative pathogen, assess potential transmission risks, and implement effective control and prevention measures.

Methods: We integrated comprehensive on-site epidemiological investigations, clinical symptom analyses, and laboratory diagnostics to isolate and identify pathogenic agents from retained food samples, environmental specimens, and anal swabs collected from affected cases. The recovered isolates underwent enterotoxin-virulence-gene profiling, antimicrobial-susceptibility testing, and phylogenetic analyses. Additionally, we characterized the architecture of the enterotoxin-A-linked pathogenicity island vSaβ.

Results: A total of 4 *S. aureus* strains were successfully isolated from 22 leftover food samples, 2 environmental swabs, and 2 patient anal swabs. Contaminated donkey and goose meat was identified as the outbreak source. All isolates harbored *sea* and *seb* enterotoxin genes, exhibited PEN-OXA-ERY-CLI resistance patterns, and were identified as clonal ST59-spa t441-SCC*mec* IVa CA-MRSA strains. Phylogenetic analysis positioned the outbreak strains within the Asia-Pacific clade, distinguishing them from the North American ST59 sublineage. Comprehensive analysis of the *sea*-associated virulence island vSaβ identified a novel structural arrangement containing a type A IEC cluster (*sea-sak-chp-scn*).

Conclusions: The detection of foodborne ST59 CA-MRSA clones in this outbreak underscores the prevalence and transmission risks associated with this hypervirulent lineage. These findings emphasize the

critical need to strengthen surveillance measures for CA-MRSA among food industry workers.

On September 16, 2024, a district CDC in Puyang City received notification of a suspected foodborne disease outbreak involving 14 individuals who developed nausea, vomiting, and diarrhea following attendance at a hotel banquet. Upon receiving this report, the District CDC immediately deployed a specialized investigation team to characterize the epidemiological features of the outbreak, identify the causative pathogen, evaluate potential transmission risks, and implement comprehensive control and prevention measures.

INVESTIGATION AND RESULTS

At 19:50 on September 16, 2024, the district CDC received notification from the Puyang City Health Commission regarding a suspected foodborne illness outbreak that had occurred during a hotel banquet at 12:00 that day. Investigation revealed that 70 individuals attended the banquet, of whom 14 subsequently developed illness. Among the affected individuals, 2 patients required hospitalization, 10 received outpatient treatment (2 with intravenous infusions and 8 with oral medication), and 2 with mild symptoms required no treatment. All patients exhibited symptom onset before 23:00 on September 16, 2024. The estimated incubation period was 4 hours, with detailed case onset times presented inSupplementary Table S1 and Figure S1 (available athttps://weekly.chinacdc.cn/). The affected population comprised 10 males and 4 females, with ages ranging from 6 to 55 years; notably, 71.4% of cases occurred in individuals aged 7–14 years. A total of 26 samples (Supplementary Table S2, available at https://weekly.chinacdc.cn/) were collected for laboratory analysis, including 22 leftover food samples, 2 environmental samples, and 2 anal swabs from patients, all submitted to Puyang CDC on September 17.

Rapid screening via multiplex fluorescence polymerase chain reaction (PCR) identified *S. aureus*-specific nucleic acids in 4 samples (Supplementary Table S2): 2 food samples and 2 anal swabs from patients (patient 1 and patient 5). Following the guidelines of GB 4789.10-2016 (National Food Safety Standards, Food Microbiology Inspection, *Staphylococcus aureus* Test) (*1*) and WS/T 80-1996 (Diagnostic Criteria and Principles of Management for Food Poisoning of *Staphylococcus aureus*) (*2*), these 4 samples underwent enrichment culture, strain isolation, Gram staining, and plasma coagulase testing. The suspected strains were confirmed as *S. aureus* through MALDI-TOF MS (Supplementary Table S2). Four *S. aureus* strains were isolated from the 4 positive samples. Fluorescent PCR assay identified the *sea* and *seb* enterotoxin genes in all 4 strains. Additionally, enzyme-linked immunosorbent assay (ELISA) detected the secreted forms of enterotoxins A and B in the culture medium (BHI) of these strains. Antimicrobial susceptibility testing using VITEK 2 Compact revealed that all 4 strains exhibited resistance to penicillin (PEN), oxacillin (OXA), erythromycin (ERY), and clindamycin (CLI). The results are presented in Figure 1A.

Whole-genome sequencing was conducted on 4

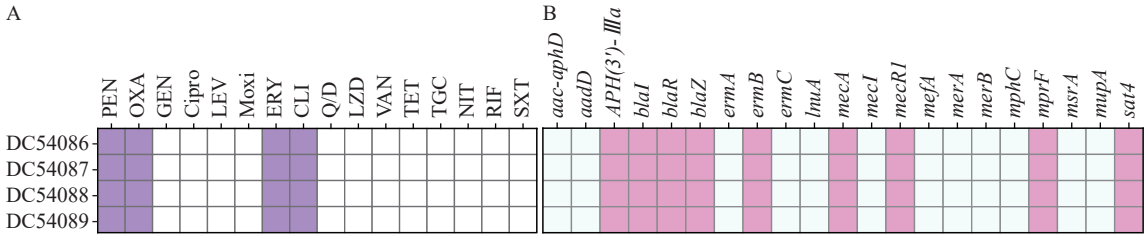

FIGURE 1. Distribution of antimicrobial resistance genes and virulence factors in four ST59 *S. aureus* isolates. (A) Heat maps display antibiotic susceptibility profiles across all strains; (B) Antimicrobial resistance gene distributions across all strains.

Note: White blocks indicate antibiotic susceptibility or gene absence, while colored blocks represent antibiotic resistance or gene presence.

Abbreviation: PEN=penicillin; OXA=oxacillin; GEN=gentamicin; Cipro=Ciprofloxacin; LEV=levofloxacin; Moxi=moxifloxacin; ERY=erythromycin; CLI=clindamycin; Q/D=quinupristin/dalfopristin; LZD=linezolid; VAN=vancomycin; TET=tetracycline; TGC=tigecycline; NIT=nitrofurantoin; RIF=rifampin; SXT=trimethoprim/sulfamethoxazole.

isolates: 3 strains underwent next-generation sequencing (NGS) analysis, while 1 strain (DC54089) was characterized using third-generation sequencing (TGS). The DC54089 genome comprised 3,444,506 bp (GC content: 36.05%) and contained 1 circular chromosome (harboring the *sea* and *seb* genes) along with 2 circular plasmids, collectively encoding 3,104 coding DNA sequences (CDS). All 4 strains shared identical origins and were confirmed as ST59-*spa* t441-SCC*mec* IVa clones, exhibiting matching antibiotic resistance and virulence gene profiles. Multiple resistance genes were detected, including *mecA*, *ermB*, *blaZ*, and *APH(3')-IIIa* (Figure 1B). Additionally, virulence genes encoding hemolysins, capsule synthesis proteins, adhesion factors, Panton–Valentine Leukocidin (PVL) toxin, exoenzymes, enterotoxins (*sea*, *seb*, *seq*, *sek*), and immune evasion cluster (IEC) components (*scn*, *sak*, and *chp*) were identified (Figure 2), demonstrating substantial pathogenic potential.

Core genome single nucleotide polymorphisms (SNPs) were identified across the 4 strains, and phylogenetic analysis was performed on the genomic sequences of these outbreak strains alongside 103 *S. aureus* ST59 reference strains using Snippy (version 4.6.0, Melbourne, Australia) (*3*). The phylogenetic tree (Figure 3) revealed that all outbreak strains isolated from food matrices clustered together with those from human samples within the same evolutionary branch (Clade China-II-I). Moreover, the staphylococcal food poisoning (SFP) strains from Henan Province formed a distinct branch (Clade Henan MRSA). Core-genome multilocus sequence typing (cgMLST) analysis demonstrated that strain DC54087 clustered tightly with the other 3 strains (DC54086, DC54088, and DC54089), differing by only a single allelic locus (≤10 alleles). These findings collectively confirm that the 4 outbreak strains originated from a common source. Detailed analysis of the *sea*-associated virulence island *vSaβ* revealed structural divergence compared to 6 reference ST59 SCC*mec* variants (Figure 4). Collinearity analysis using Easyfig (version 2.2.5, Brisbane, Australia) identified a type A IEC gene cluster (*sea-scn-sak-chp*) with partial deletions in the *ΦSa3* gene. Two copies of *scn* and distinct rearrangements of the *chp* and *scn* loci revealed a novel gene sequence within the *vSaβ* region. Based on clinical symptoms, epidemiological evidence, laboratory findings, and genomic analysis, this outbreak was determined to be a foodborne illness caused by ST59-*spa* t441-SCC*mec* IVa MRSA producing enterotoxins A and B.

PUBLIC HEALTH RESPONSE

Following these findings, the District CDC implemented comprehensive public health interventions: 1) conducted thorough disinfection of cold dish storage areas, cutting boards, and knives; 2) ensured safe disposal of all remaining food items; 3) mandated immediate self-inspection protocols within the affected hotel; 4) provided enhanced food safety training for all employees, emphasizing proper food processing techniques, rigorous hand hygiene practices, and effective disinfection protocols.

DISCUSSION

Staphylococcus aureus represents a clinically significant pathogen frequently implicated in foodborne intoxication events. This organism produces over 29 distinct staphylococcal enterotoxins (SEs) and staphylococcal enterotoxin-like (SEl) toxins. Among these, SEA, SEB, SEC, SED, and SEE constitute the most prevalent enterotoxins, collectively accounting for approximately 95% of SFP outbreaks globally (*4*).

The SFP outbreak documented in Puyang City resulted from contamination of donkey and goose meat (served as cold mixed dishes) with *S. aureus*

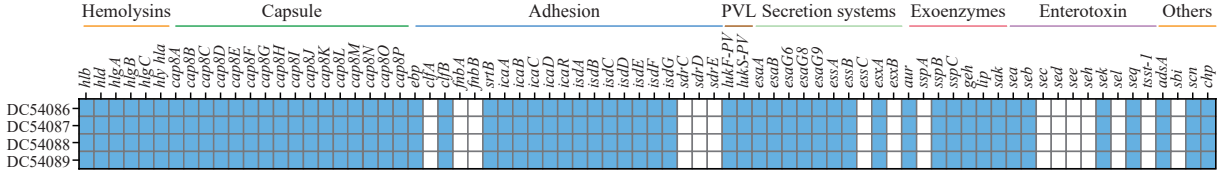

FIGURE 2. Virulence gene profiles and genetic variations across the four outbreak strains.
Note: White blocks denote gene absence, while colored blocks indicate gene presence. The horizontal color bar (left to right) represents genes associated with hemolysins, capsule formation, adhesion factors, PVL, secretion systems, exoenzymes, enterotoxins, and additional virulence determinants.
Abbreviation: PVL=panton-valentine leucocidin.

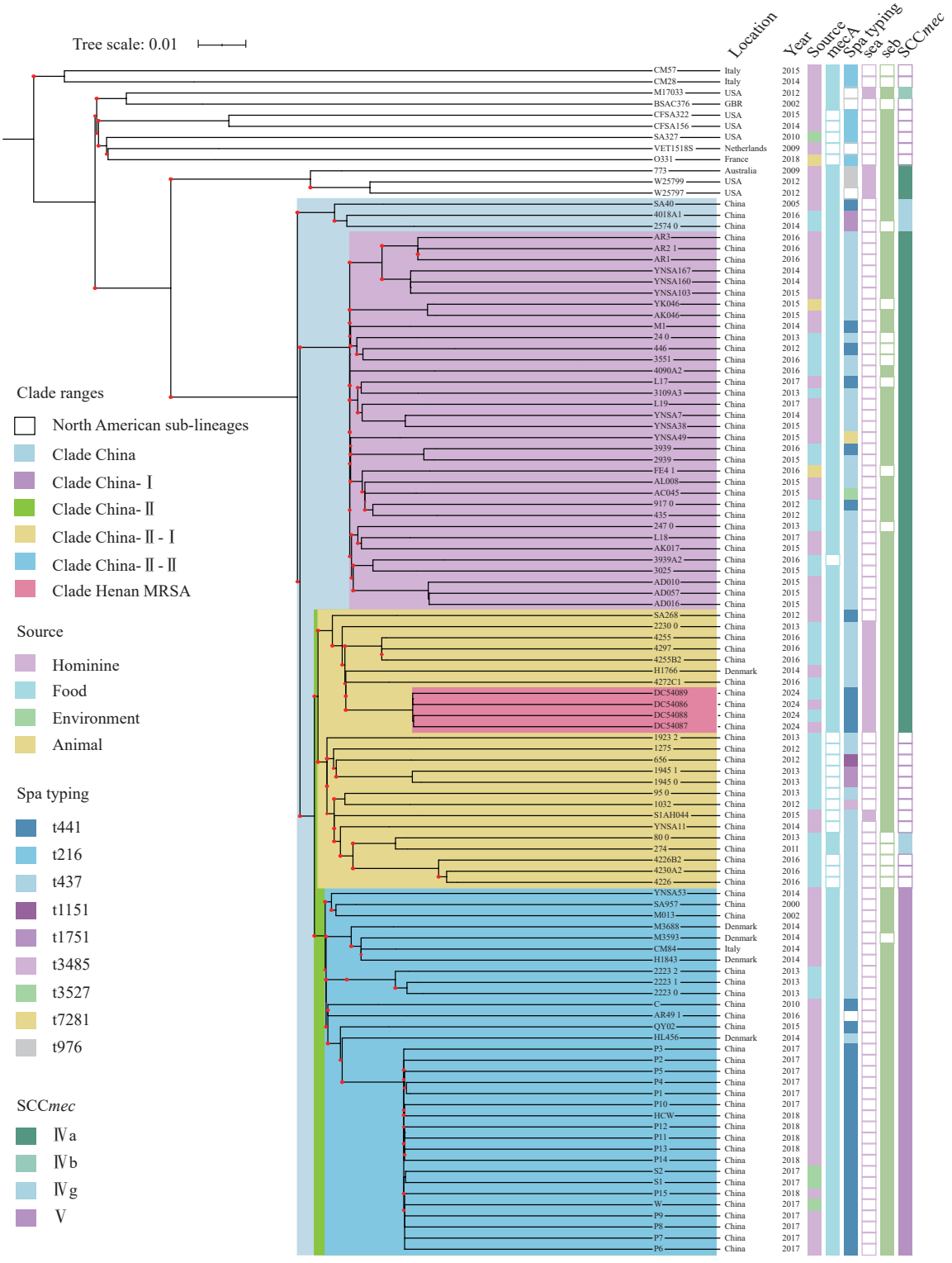

FIGURE 3. Phylogenetic reconstruction of the ST59 lineages.
Note: A total of 107 ST59 sequences (4 from this study and 103 from the NCBI database) were analyzed. The Henan MRSA ST59 isolates are shown in red. The reference genome is the completely sequenced ST59 MRSA isolate M013 (NCBI BioSample accession: CP003166). The filled squares indicate the presence of individual genes, while the empty squares indicate their absence, as specified at the top of each column. The clade ranges, sources, *spa* types, and SCC*mec* types of 107 strains have been presented on the left side.
Abbreviation: MRSA=methicillin-resistant *Staphylococcus aureus*; SCC*mec* types=*Staphylococcal* cassette chromosome *mec* types.

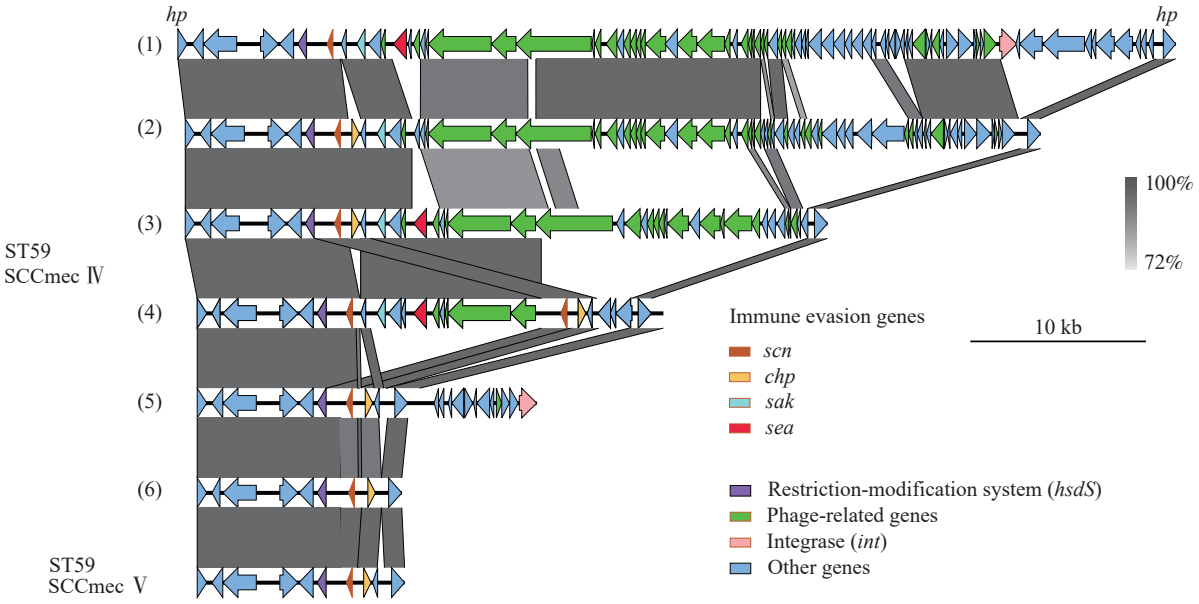

FIGURE 4. Comparison of genomic island (*vSaβ*) among ST59 isolates with different SCC*mec* types.
Note: Arrows and arrowheads represent open reading frames (ORFs) and the direction of transcription. The nucleotide similarities in the structure are indicated by grey shading. No. (4) represents the Henan representative strain DC54089.

enterotoxins A and B. This determination was substantiated through comprehensive epidemiological evidence, clinical symptom analysis, and laboratory findings. Multiple lines of evidence supported this conclusion: 1) all affected individuals shared exposure to a single hotel banquet; 2) symptom onset occurred synchronously within a 12-hour window (Supplementary Figure S1), consistent with the characteristic incubation period for SFP; 3) patients presented with uniform clinical manifestations, predominantly nausea and vomiting with or without diarrhea, which are pathognomonic for SFP; 4) multiplex fluorescence PCR and bacterial culture successfully identified *S. aureus* in specimens from two patients and two food samples. The four isolated strains demonstrated the capacity to produce enterotoxins A and B. Phylogenetic analysis of these SFP strain genomes (Clade Henan MRSA) alongside 103 ST59 sequences revealed that the outbreak strains clustered within Clade China-II-I, a lineage predominantly comprising strains of food origin. The two contaminated food items were identified as chilled donkey meat and chilled Cantonese-style roast goose. However, the absence of specimens from kitchen staff or the processing environment precluded definitive identification of the contamination source.

Currently, ST6, ST7, ST943, ST5, ST2315, ST15, ST59, and ST7591 represent the predominant causative strains of SFP in China, with most demonstrating methicillin sensitivity (*5*–*8*). Our investigation identified the ST59-t441 SEA/SEB-positive MRSA strain as the causative agent, marking the first documented SFP outbreak in Henan Province. This finding aligns with retrospective analyses demonstrating that ST59 constitutes the primary MRSA type responsible for food poisoning outbreaks across multiple Chinese cities, including Shijiazhuang, Suzhou, and locations throughout Sichuan Province (*6*–*8*). Furthermore, ST59 has emerged as the most prevalent CA-MRSA strain isolated from Eastern Asian communities and has established dominance in healthcare settings over the past two decades (*9*).

Phylogenetic analysis demonstrated that the SFP outbreak strains exhibited distant genetic relationships with North American sub-lineages while clustering closely with ST59 MRSA strains isolated from food and human samples throughout China, confirming their classification within the Asia-Pacific clone. Within the phylogenetic tree, most Chinese ST59 strains carried *seb*, whereas only strains within Clade China-II-I and North American sub-lineages harbored both *sea* and *seb* genes (Figure 3). All ST59-t441 MRSA isolates detected in this investigation carried the characteristic human IEC genes *scn*, *sak*, and *chp*, indicating their potential association with human hosts. Unfortunately, the absence of specimens from kitchen staff prevented determination of the outbreak source.

ST59 strains commonly exhibit elevated prevalence of the *seb*, *seq*, and *sek* genes. In this outbreak, the ST59-t441 MRSA strains harbored both *sea* and *seb* genes and actively secreted enterotoxins A and B *in vitro*. The synergistic action of these dual toxins likely accounts for the severe clinical manifestations and subsequent hospitalization observed in several patients. Structural analysis of the *sea*-associated virulence island *vSaβ* identified a previously unreported configuration featuring a type A IEC cluster (*sea-sak-chp-scn*). Consistent with earlier findings, genetic environment analysis indicated that the ST59-t441 MRSA strains from this outbreak lacked the characteristic *ν Saβ* structure due to staphylococcal prophage ΦSA3 insertion (*10*). Within these ST59-t441 MRSA strains, certain ΦSA3-related genes were absent, while two copies of the *scn* gene were detected. The functional implications of these genomic alterations on strain pathogenicity and horizontal *sea* transfer warrant additional investigation.

The detection of foodborne ST59 CA-MRSA clones in this outbreak underscores both the widespread distribution and transmission potential of this hypervirulent lineage. To support comprehensive risk assessment efforts, we recommend strengthening surveillance protocols for CA-MRSA among healthy populations, with a particular emphasis on food industry workers.

Conflicts of interest: No conflicts of interest.

doi: 10.46234/ccdcw2025.184

[#] Corresponding authors: Xiaomei Yan, yanxiaomei@icdc.cn; Qingjie Zhang, pycdczqj@163.com.

[1] Puyang Key Laboratory for Infectious Disease Prevention and Control, Puyang Center for Disease Control and Prevention, Puyang City, Henan Province, China; [2] National Key Laboratory for Intelligent Tracking and Forecasting for Infectious Diseases, National Institute for Communicable Disease Control and Prevention, Chinese Center for Disease Control and Prevention, Beijing, China; [3] Henan Provincial Center for Disease Control and Prevention, Zhengzhou City, Henan Province, China.

[&] Joint first authors.

Submitted: May 19, 2025
Accepted: August 05, 2025
Issued: August 15, 2025

REFERENCES

1. The National Health and Family Planning Commission of the People's Republic of China, National Medical Products Administration. GB 4789. 10-2016 National standard for food safety microbiological examination of *Staphylococcus aureus*. Beijing: Standards Press of China, 2017. http://www.csres.com/detail/293953.htmlhttps://sppt.cfsa.net.cn:8086/db. (In Chinese).
2. Health Supervision Department of the Ministry of Health National Health Commission of the People's Republic of China. WS/T 80-1996 Diagnostic criteria and principles of management for food poisoning of *Staphlococcus Staphylococcus aureus*. : , 1997. https://www.antpedia.com/standard/1018774.html. (In Chinese).
3. Zou G, Matuszewska M, Bai FL, Wang SY, Wang S, Li HX, et al. Genomic analyses of *Staphylococcus aureus* isolated from yaks in Ganzi Tibetan Autonomous Prefecture, China. J Antimicrob Chemother 2022;77(4):910 – 20. https://doi.org/10.1093/jac/dkac011.
4. Hennekinne JA, De Buyser ML, Dragacci S. *Staphylococcus aureus* and its food poisoning toxins: characterization and outbreak investigation. FEMS Microbiol Rev 2012;36(4):815 – 36. https://doi.org/10.1111/j.1574-6976.2011.00311.x.
5. Li GH, Wu SZ, Luo W, Su YL, Luan Y, Wang X. *Staphylococcus aureus* ST6-t701 isolates from food-poisoning outbreaks (2006-2013) in Xi'an, China. Foodborne Pathog Dis 2015;12(3):203 – 6. https://doi.org/10.1089/fpd.2014.1850.
6. Lv GP, Jiang RP, Zhang H, Wang L, Li LJ, Gao WL, et al. Molecular characteristics of *Staphylococcus aureus* from food samples and food poisoning outbreaks in Shijiazhuang, China. Front Microbiol 2021;12:652276. https://doi.org/10.3389/fmicb.2021.652276.
7. Zheng J, Liu L, Chen G, Xu WP, Huang YL, Lei GP, et al. Molecular characteristics of *Staphylococcus aureus* isolates form food-poisoning outbreaks (2011-2022) in Sichuan Province, China. Foodborne Pathog Dis 2024;21(5):323 – 30. https://doi.org/10.1089/fpd.2023.0097.
8. Yu SY, Zhou YX, Feng D, Jiang QG, Li TL, Jiang GL, et al. Whole genome sequence-based characterization of virulence and antimicrobial resistance gene profiles of *Staphylococcus aureus* isolated from food poisoning incidents in eastern China. Front Microbiol 2023;14:1225472. https://doi.org/10.3389/fmicb.2023.1225472.
9. Wang BJ, Xu YL, Zhao HL, Wang XY, Rao LL, Guo YJ, et al. Methicillin-resistant *Staphylococcus aureus* in China: a multicentre longitudinal study and whole-genome sequencing. Emerg Microbes Infect 2022;11(1):532 – 42. https://doi.org/10.1080/22221751.2022.2032373.
10. Jin Y, Zhou WX, Zhan Q, Zheng BW, Chen YB, Luo QX, et al. Genomic epidemiology and characterization of methicillin-resistant *Staphylococcus aureus* from bloodstream infections in China. mSystems 2021;6(6):e00837 – 21. https://doi.org/10.1128/mSystems.00837-21.

SUPPLEMENTARY MATERIAL

SUPPLEMENTARY TABLE S1. The basic information, clinical symptoms and treatment of 14 patients by onset time.

Patients	Sex	Age (years)	Onset time	Clinical symptoms	Treatment
Patient 1	Male	7	15:00, Sep 16	Vomiting (6 times), diarrhea (3 times)	Hospitalization,
Patient 2	Male	12	15:00, Sep 16	Vomiting (8 times), diarrhea (5 times)	Outpatient oral medication
Patient 3	Male	12	15:00, Sep 16	Vomiting (2 times)	Outpatient oral medication
Patient 4	Male	40	15:00, Sep 16	Nausea, diarrhea (4 times)	Outpatient oral medication
Patient 5	Male	7	15:30, Sep 16	Vomiting (8 times), diarrhea (3 times)	Hospitalization
Patient 6	Male	40	16:00, Sep 16	Vomiting (3 times)	Outpatient oral medication
Patient 7	Male	6	16:00, Sep 16	Nausea	Untreated
Patient 8	Female	12	16:00, Sep 16	Nausea, vomiting (1 time)	Untreated
Patient 9	Female	12	16:00, Sep 16	Nausea, diarrhea (3 times)	Outpatient oral medication
Patient 10	Male	13	16:00, Sep 16	Nausea, vomiting (5 times)	Outpatient oral medication
Patient 11	Female	37	−, Sep 16	Vomiting (multiple times), diarrhea (multiple times)	Outpatient intravenous infusion
Patient 12	Female	53	−, Sep 16	−	Outpatient intravenous infusion
Patient 13	Male	14	−, Sep 16	Vomiting (3 times), diarrhea (3 times)	Outpatient oral medication
Patient 14	Male	13	−, Sep 16	Vomiting (3 times), diarrhea (2 times)	Outpatient oral medication

Note: "−" means unrecorded.

SUPPLEMENTARY TABLE 2. The information and test results of the 26 samples.

Sample source	Sample name	Multiplex fluorescence PCR	MALDI-TOF MS	Enterotoxins gene	Enterotoxins protein	Strain ID
Patient	Anal swab 1 (Patient 5)	*S. aureus*	*S. aureus*	*sea*, *seb*	SEA, SEB	DC54086
	Anal swab 2 (Patient 1)	*S. aureus*	*S. aureus*	*sea*, *seb*	SEA, SEB	DC54087
Leftover food	Donkey meat	*S. aureus*	*S. aureus*	*sea*, *seb*	SEA, SEB	DC54088
	Cantonese roast goose	*S. aureus*	*S. aureus*	*sea*, *seb*	SEA, SEB	DC54089
	Five blessings platter, Scallion and beef tripe salad, Daokou braised chicken, Yam vermicelli, Crisp and refreshing celery, Secret recipe water chestnut, Dalian live abalone, Steam pot seafood shrimp, Steamed deep-sea flounder, Lucky braised pig's face, Beijing roast duck with fruit wood, Stewed turtle with old hen, Garlic-topped steamed scallops, Caterpillar fungus stuffed lion's head, Mildly spicy lamb with green peppers, Pumpkin wrapped eight treasures, Cantonese style morning glory, Guihe big steamed buns, Red date flavored steamed sponge cake, Small cake	Negative	No	No	No	No
Environment	Chopping board and Kitchen knife	Negative	No	No	No	No

Abbreviation: MALDI-TOF MS=Matrix-Assisted laser desorption/ionization time-of-flight mass spectrometry.

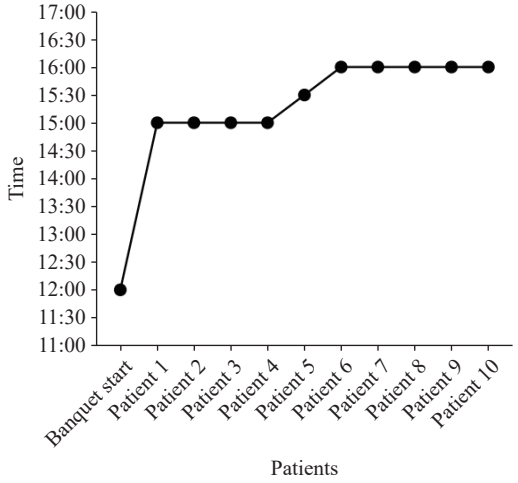

SUPPLEMENTARY FIGURE S1. Epidemic curve displaying patient onset times.
Note: Onset times for patients 11–14 were not recorded.

Youth Editorial Board

Indexed by Science Citation Index Expanded (SCIE), Social Sciences Citation Index (SSCI), PubMed Central (PMC), Scopus, Chinese Scientific and Technical Papers and Citations, and Chinese Science Citation Database (CSCD)

The inauguration of *China CDC Weekly* is in part supported by Project for Enhancing International Impact of China STM Journals Category D (PIIJ2-D-04-(2018)) of China Association for Science and Technology (CAST).

CCDC weekly

Vol. 7 No. 33 Aug. 15, 2025

Responsible Authority
National Disease Control and Prevention Administration

Sponsor
Chinese Center for Disease Control and Prevention

Editing and Publishing
China CDC Weekly Editorial Office
No.155 Changbai Road, Changping District, Beijing, China
Tel: 86-10-63150501, 63150701
Email: weekly@chinacdc.cn

CSSN
ISSN 2096-7071 (Print)
ISSN 2096-3101 (Online)
CN 10-1629/R1